2019

Master Materials Engineering and Energy
Module Ceramics and Glass



DEPARTMENT OF CHEMISTRY

SEMESTER II

Module : Ceramics and Glasss

Specialty
Master Materials Engineering and Energy

Controls on Ceramics

Pr. Saïd BENMOKHTAR

FACULTÉ DES SCIENCES BEN M'SIK - CASABLANCA
Pr. Saïd BENMOKHTAR
Tel :**06 68 55 78 19**
Fax :**05-22-70-46-75**
Adresse :**Avenue Cdt,Driss el harti B.P: 7955 -Ben M'Sik**

Avant-propos

Ce polycopie regroupe des exercices de *Chimie des solides spécialement sur les céramiques enseigné en Master des Matériaux*. La plupart des sujets proposés présentent un aspect pratique. Les exercices présentés mettent l'accent sur l'importance fondamentale de cette matière, de plus en plus négligée. J'ai également développé les réactions de synthèse.

Il s'inscrit dans l'évolution et l'enrichissement continuel sur les céramiques et qu'il témoigne de sa vitalité et de son enrichissement. Loin d'être un domaine standardisé, il n'est plus non plus à ses débuts et son exposition s'est enrichie au fur et à mesure de l'expérience acquise en l'enseignant à l'enseignement universitaire en Master (Option Matériaux).

Il représente un choix pragmatique fondé sur un enseignement réalisé en interaction avec des étudiants. C'est un choix original de sujets et il dévoile au fil des pages les prolongements des éléments de base vers des sujets plus spécialisés. En ce sens, il constitue une introduction stimulante, qui donne envie d'aller plus loin aux débutants et réserve des surprises aux spécialistes du domaine. Il plaira spécialement aux étudiants ayant le goût des céramiques modernes.

En conclusion, J'ai fait appel à un grand nombre de ces exercices, qui proviennent de résultats expérimentaux issus de la recherche en particulier des articles publiés.

Pr. Saïd BENMOKHTAR

Materials Research Bulletin 47 (……) 1954–1960



Contents lists available at SciVerse ScienceDirect
Materials Research Bulletin
Journal home page:www.elsevier.com/locate/matresbu



Title:
………..…………………………………………………………………
………………
…………………………………………………………………………
……………………

G. Delaizir [a,*], G. Bernard-Granger [b], J. Monnier [a], R. Grodzki [a], O. Kim-Hak [c], P.-D. Szkutnik [b], M. Soulier [b],
S. Saunier [c], D. Goeuriot [c], O. Rouleau [a], J. Simon [b], C. Godart [a], C. Navone [b]

[a] *Institut de Chimie et des Matériaux Paris Est (ICMPE-CNRS), UMR 7182, 2 rue Henri Dunant, 94320 Thiais, France*
[b] *Laboratoire des Composants pour la Récupération d'Energie, CEA/LITEN/LCRE, 17 rue des Martyrs, 38054 Grenoble, France*
[c] *Centre Sciences des Matériaux et des Structures, de l'Ecole Nationale des Mines de Saint-Etienne, 158 Cours Fauriel, 42023 Saint-Etienne, France*

ARTICLE INFO

Article history:
Received 28 July 2011
Received in revised form 1 March 2012 Accepted 12 April 2012
Available online 23 April 2012

Keywords:
……………………
……………………
……………………
……………………
……………………

ABSTRACT

…………………………………………………………………………
…………………………………………………………………………
…………………………………………………………………………
…………………………………………………………………………..
…………………………………………………………………………
…………………………………………………………………………
…………………………………………………………………………
…………………………………………………………………………..
…………………………………………………………………………
…………………………………………………………………………

1. Introduction

In an energy context saving, thermoelectric materials that are able ……………………………………........ ……and vice versa have attracted extensive interest. Applications of such thermoelectric devices range from exhaust waste heat recovery system attached to the hot area (exhaust pipe, radiator) of cars or power generator in space applications for example for refrigeration [1–5]. Efficiency of thermoelectric materials is defined by its figure of merit ZT = ($S^2\sigma T/\lambda$) where S is the …………………, σ the …………………, T the …………………, λ the ………………… and $S^2\sigma$ is the …………………

Among all thermoelectric materials, bismuth telluride (………..) is one of the key materials for room temperature applications. Since the mid 1950s, its figure of merit ZT has improved considerably to reach the highest value of 1.56 at 300 K for a p- type bulk ………. [6]. This last value has been obtained with nanostructured composite materials taking advantage of the phonon scattering in these materials and leading to lower thermal conductivity.

Moreover, it is also well known that the processing parameters influence the thermoelectric properties for one given material [7,8]. In this paper, we investigate the sintering of p-type nanopowder, ……………………………………………. ..……..……………………………………… ………...…………………………………… …………...………………………………… ……………………………………………… ……… ……..………………………………………… …

First, …………………………………………… ….. …….. …………………………………………… ….. …….. …………………………………………… ….. …………………………………………… ………... It is a non-conventional sintering technique based on the use of pulsed current, ……………… heating (up to 600 °C/min) and cooling rates, and lower sintering temperatures are often observed in comparison with conventional sintering techniques [12–14]. The interest of the scientific community for this technique grows rapidly for its great advantages namely, …………………, the …………………….. the sintered ceramics, the ………………….. of nanostructure of the initial powder into the sintered ceramics due to the fast heating rate and also the ease of transfer to industry.

The second non-conventional sintering technique is ……………………... This rapid sintering process has shown spectacular results with the densification of several ceramic materials [15]. The main advantage of this process is the possibility to obtain ………………………… due to the very low sintering time at low temperature. Recent study has shown promising results on p-type bismuth telluride [16].

Finally, the conventional …………………………. technique has been used to compare the results with the two previous sintering techniques in terms of microstructure and thermoelectric properties. Like the ………, this technique is also currently used in industrial process.

2. Experimental

2.1. Powder synthesis

p-Type bismuth telluride (…………………..) is synthesized by mechanical alloying (MA) in a planetary ball milling equipment using appropriate amount of high purity ………….. (Alfa, 99.999%), …………. (Sigma–Aldrich, 99.999%) and ………….. (Sigma–Aldrich,

99.999%) powders. Powders were charged into a hardened steel vial with a ball-to-powder weight ratio of
20:1 and sealed in an argon atmosphere to prevent the oxidation during MA process. The central shaft rotation rate was as high as 400 rpm during 9 h:30.

2.2. Sintering techniques

2.2.1. ……………………………..

All the …….. tests are conducted under vacuum using the equipment Dr. Sinter 515S Syntex machine located in CNRS Thiais, France.
The p-type ……….. powder (typical batch of 1.5 g) is introduced into a Ø 8 mm carbon die with a layer of protective papyex, without any previous pre-shaping. The system is closed by carbon punches at both sides which transmit the uniaxial pressure. DC pulses are delivered to the die by the punches allowing the temperature to rise rapidly (about 100 °C/min). The temperature is controlled via a …………….. located into the wall of the die which adjusts the power output. In the present case, the temperature has been increased up to a maximum of 360 °C.
The soak time, when the temperature of reaction is reached,
namely 360 °C, is 5 min under a load of 50 MPa.

2.2.2. ………………….

Densification of p-type ……….. powder is performed by microwave hybrid heating in a specifically designed crucible (Ø 8 mm) located in a 430 mm ×430 mm × 490 mm multimode cavity under nitrogen atmosphere (PN_2 = 1 bar). It comprises silicon carbide (SiC) barrels regularly arranged around the sample. This design allows a homogenous heating of the inner cavity. The applied microwave power was 600 W with a frequency of 2.45 GHz. The temperature of the surface of the sample is read by an optical pyrometer located on the top of the cavity. A heating rate of 100 °C/min can then be reached with a very good reproducibility. The maximum sintering temperature ranges from 400 to 420 °C for the different tests and the soak duration is 10 min. It is noteworthy that for these temperatures, little evaporation of tellurium is observed on the top of the crucible; EDX analysis proves that this deposition is mainly tellurium.

2.2.3. ………………………………..

p-Type …………. powder is first consolidated by cold compaction at 70 MPa under …………. atmosphere and packed into a Ø 10 mm copper cylinder. The thermocouple is located close to the cylinder containing the sample. The cylinder was then welded under vacuum and compressed by ……………………………. using the following conditions: 480 °C for 60 min with a mean isostatic stress of 140 MPa.

2.3. Characterizations

After the different …………………..., density of pellets was determined by the ………………….. method. Microstructure of pellets as well as chemical composition was determined by …………………. (SEM FEG, LEO 1530 equipped with Energy-dispersive X-ray spectroscopy, EDX) and ……………………………. (MET, JEOL 2000Fx) operated at 200 kV. X-Ray Diffraction (XRD) was performed using a D8 Bruker equipment.

2.3.1. Harman method

Usually ZT is determined thanks to individual measurements of the ……………….. coefficient S, the ………………………σ and the ……………….. λ. The Harman method allows measuring directly ZT without these three factors with only one measurement, in adiabatic conditions, from resistivity measurements in alternative and direct currents as described as follows. When a direct current is applied to a thermoelectric material, Peltier effect is established:
Qp = S × T × idc (Qp: heat exchange between the ends of material, idc: direct current). In adiabatic conditions, heat exchange by diffusion (Q_d) is compensated by heat transported by Peltier effect:
$Q_p + Q_d = 0$ (with $Q_d = \lambda \times S_{urf} \times \Delta l/l$;
S_{urf}: section of

sample, l: length of sample). So we have

$$S \times T \times i_{dc} = \lambda \times S_{urf} \times \Delta T/l :$$

Due to Seebeck and Ohm effects:

$V_{dc} = R \times i_{dc} + S \times DT = \rho \times l \times i_{dc}/S_{urf} + S^2 \times T \times i_{dc} \times 1/\lambda \times S_{urf}$

Now, with a high frequency alternative current iac, thermal gradient cannot establish, so there is no Seebeck potential but ohmic drop persists and then: $V_{ac} = R \times i_{dc} = \rho \times l \times i_{ac}/S_{urf}$ with R the resistance of the material. Assuming $i_{dc} = i_{ac} = i$, we have:

$$\frac{v_{dc} - v_{ac}}{v_{ac}} = \frac{S^2 \times T}{\lambda \times \rho} = \frac{S^2 \times T \times \sigma}{\lambda} = ZT$$

If $i_{dc} \neq i_{ac}$: replacing V_{dc}/i_{dc} by R_{dc} and V_{ac}/i_{ac} by R_{ac} leads to $ZT = R_{dc} - R_{ac}/R_{ac}$. Current and potential manganin wires are welded to the sample thanks to indium contacts and are connected to sample holder. The setup is connected to PPMS (Quantum Design) for ac-current and to a home-made resistivity set-up for dc-current. The experimental enclosure is vacuumed to keep adiabatic conditions at room temperature.

2.3.2. Measurements of S, σ and λ

The ………….. coefficient, S, is measured by a home-made apparatus where the differential temperature is obtained by maintaining a cold part (288K) and heating the second one at room temperature. …………coefficient is calculated by the ratio of the Seebeck voltage and the differential temperature. ……………………. σ was measured using a Four-Point Probe method and the carrier concentration and mobility were determined by an Ecopia Hall effect measurement at room temperature (HMS-3000 apparatus). …………………………., λ, is deduced from the ZT, S and s measurements according to the following equation:

$$ZT = \frac{S^2 \sigma T}{\lambda}$$

3. Results and discussion

The sintering parameters (temperature, pressure and power) for the …………… techniques have been optimized to get high compactness. The almost full density (≥97%) has been reached for ……. and ……… techniques while only ~90% compactness is the maximum for the ceramic processed by …………………. (Table 1).

Table 1: Physical characterizations of the p-type …………. ceramics processed by ………, …….. and ……………….

Sintering technique	Compactness	Electrical conductivity (S/m)[a]	Seebeck coefficient (μV/K)[a]	Charge carriers (cm^3)	Mobility (cm^2/Vs)	Power factor (W/mK^2)[b]	Thermal conductivity (W/mK)[a]	ZT[c]	Concentration of precipitates (precip./nm^2)[a]
	99%	60,600	221	1.5E+19	257	2.96E−3	1.29	0.68	3.1×10^{-5}
	97%	156,000	160	5.0E+19	194	4.0E−3	2.06	0.53	1.2×10^{-5}
	90.5%	49,600	230	2.3E+19	133	2.62E−3	1.06	0.74	1.6×10^{-5}

[a] Standard deviation over estimated to ±3%.
[b] Standard deviation over estimated to ±8%.
[c] Standard deviation over estimated to ±10%.

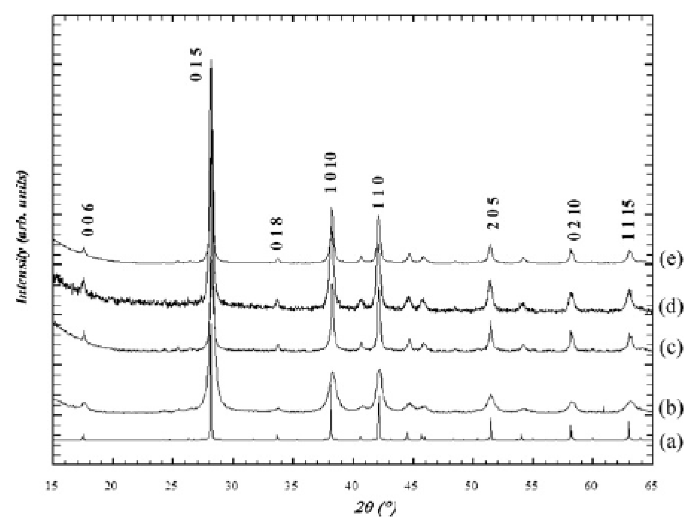


Fig. 1. XRD patterns

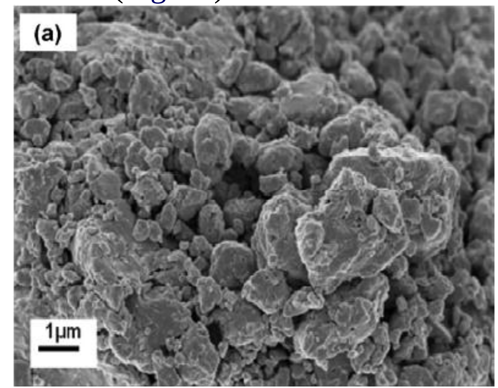
(a) (JCPDS 49-1713) of theoretical ………………
(b) initial …………………… powder
(c) ceramics processed by ……………….
(d) ceramics processed …………………..
(e) ceramics processed ……………………

Densities higher than 90% could not be obtained by …………………… due to the …………………… (EDX analysis). The …………………… is limited for the …….. and ………… sintering techniques because the sample is confined in a matrix.

XRD patterns of the …………. ceramics are similar and no significant change with the XRD pattern of the initial powder is observed (Fig. 1).

Initial p-type ………. powder is formed by agglomerates whose size (<10 mm) is rather inhomogeneous (Fig. 2a). At higher magnification, these agglomerates appear

like formed by primary particles that have nearly spherical shape and sizes in the range 20–50 nm (Fig. 2b).



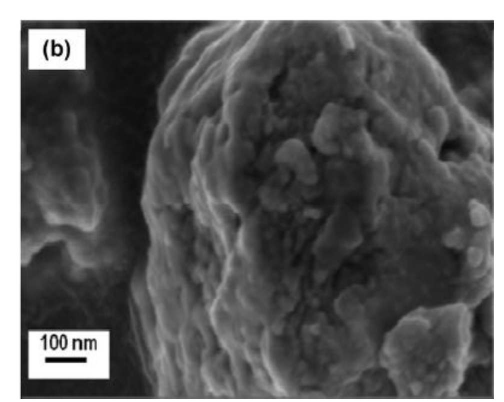


Fig. 2. ……………….. of initial p-type ………… powder (a), at higher magnification (b).

Electrical and thermal characteristics of the ceramics sintered by ……………………………………….are summed up in Table 1.

The ZT values of the ceramics processed either by ………….. are quite similar and equal to _0.7 (0.68 for ………. ceramic and 0.74 ……………………….) but this value is different from the ZT value of the ceramic processed by …………. (ZT = 0.53) (Table 1). We explain this difference in thermoelectric properties from two main contributions:

- the difference in charge carriers concentration;
- the microstructure.

According to the Ioffe theory, the relationship between …………… coefficient and the carrier concentration can be given by the following equation:

$$S \approx \gamma + \ln\frac{1}{n}$$

where S, g and n are the ………….. coefficient, the scattering factor and the charge carrier concentration, respectively. It is well known that two competing factors of carrier concentration and mobility determine the ………………………., and the relationship can be
described by the following equation:

$$\sigma = ne\mu$$

where **σ**, **μ** and e are the ……………………….., the carrier mobility and the electron charge, respectively.

The influence of sintering technique on the charge carrier concentration and the …………... coefficient is shown in Table 1. Ceramics processed by ……….. (vacuum, 50 MPa, 360 °C, 5 min dwell time) and ……………. (nitrogen, 420 °C, 10 min dwell time) sintering techniques show lower charge carriers concentration than the ceramic processed by …………. (vacuum, 140 MPa, 480 °C, 60 min dwell time). This is hypothesized to be linked to the sintering conditions (temperature, dwell time, atmosphere and pressure) and especially the sintering temperature that favors or not the creation of vacancies or anti-site defects [17] by the creation of a second phase and the evaporation of tellurium during sintering. To explain this behavior, different p-type materials …………….. with 0.9 ≤ x ≤ 1.7) have been studied. Fig. 3 ……………………………………………… …………………
……………………………………………… ……………………………………………… …………………………………….

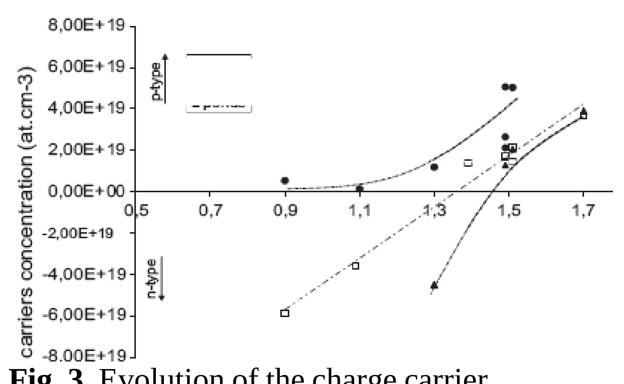


Fig. 3. Evolution of the charge carrier concentration as a function of x in …………….. for the ………….. sintering techniques (……….., …………. and ………………).

The evolution ………………………………………… …………………………............................ .... (creation of positive charge carrier). However for x less than 1.3, the material still remains n-type (the number of holes created does not compensate the number of electrons in the material). The ………… technique is well known to allow short sintering time and lower sintering temperature in comparison with ……………. techniques. These conditions can prevent the evaporation of tellurium from the material during the sintering. This directly affects the charge carrier concentration and, as a consequence, we observe a linear relationship between the amount of antimony, x, and the charge carrier concentration.

In the case of the ………………….., the alloys ………………… with $0.9 \leq x \leq 1.7$ are always p-type materials. The ………………… temperature is higher than the ………………… one (T(…….) = 480 °C and T(…….) = 360 °C) and even higher than the Bi–Te eutectic (417 °C). This probably induces the apparition of a second phase with vacancies or anti-structure defects at the origin of positive charge carriers. In p-type ………………… (or Bi_2Te_3–Sb_2Te_3) alloys, the holes are usually created by the anti-structure defects generated by the occupation of Te sites with Bi and Sb atoms, which can be described as follows [18]:

$Bi_2Te_3 = 2BiTe^{/} + 2V_{Bi}^{\times} + V_{Te} + 3/2\ Te_2(g) + 2\ h$

$Sb_2Te_3 = 2SbTe^{/} = + 2V_{Sb}^{\times} + V_{Te} + 3/2\ Te_2(g) + 2\ h$

where V_{Te} is Te vacancy and $V_{Bi\ (or\ Sb)}$ is Bi or Sb vacancy. Conversely, negative charge carriers seem to be favored in the microwave sample. This is not surprising because as previously mentioned; some tellurium evaporation is observed which is at the origin of the creation of vacancies and negative charge carrier.

For similar compactness (>97%) obtained for ceramics processed by either …….. or ……, as the charge carriers concentration increases, the electrical and the thermal conductivities increase as well for the two ceramics.

The thermal conductivity, k can be divided into two components: the lattice thermal conductivity (k_L) and the electronic thermal conductivity (k_E). The lattice thermal conductivity k_L was determined by the Wiedemann–Franz relation $k_L = k - L\sigma T$, where $L\sigma T$ is the electronic thermal conductivity, k_E, L is the Lorentz number ($L = 2.0\times10^{-8}\ V^2/K^2$ for heavily doped semi-conductor [6]), s is the electrical conductivity and T is the temperature in Kelvin. Therefore k will also be affected by the carrier concentration variation. k_E will decrease with the electrical conductivity whereas the lattice component k_L will be affected by the mass of unit cell and the grain size. At 300 K, the k_L of the ………, ……….. and ………….. samples is respectively 0.93 W m^{-1} K^{-1}, 1.12 W m^{-1} K^{-1} and 0.76 W m^{-1} K^{-1}. The ………….. sample has the lowest thermal conductivity which we assume to be linked to the low compactness.

Consequently, despite the low compactness (90%) of the ceramic processed by ……………, this one shows the highest ZT value (~0.7). This low compactness induces a very low thermal conductivity and a very low thermal lattice component k_L due to an increased scattering of phonons by pores (phonon pore-scattering effect) and the

presence of precipitates. In parallel, the low compactness induces a decrease in the electrical conductivity with a loss of charge carriers. It is noteworthy that the charge carrier concentration for this ceramic (2.3 $\times 10^{19}$ cm^{-3}) is close to the value reported by Lan et al. in the case of nano-structured materials [19].

Microstructure of ceramics processed by …………… ……………………… techniques is shown in Fig. 4. The average grain size of the ceramic sintered by ………….. ……….. (Fig. 4a and b) than the ones sintered by ……….. (Fig. 4c and d) or ……….. (Fig. 4e and f).

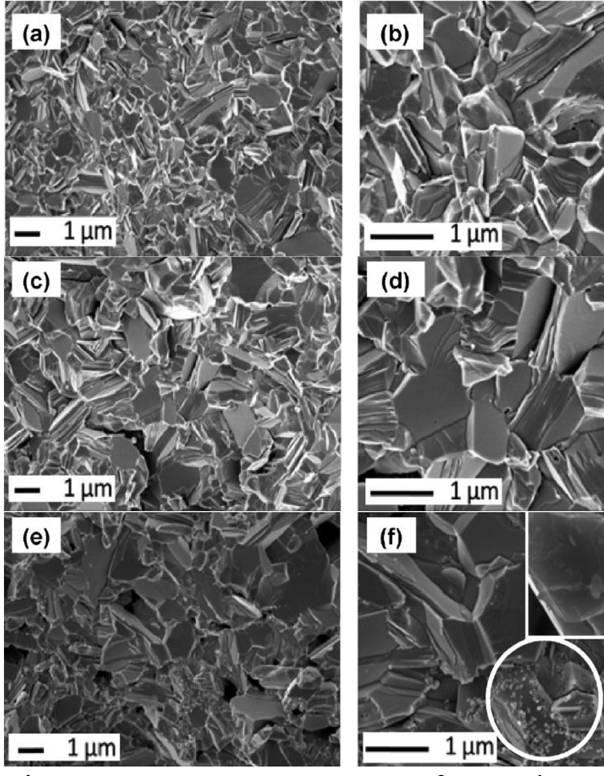


Fig. 4. ……………………… of ceramics processed by …………… (a and b), …………… (c and d) and …………… (e and f).

These results are expected because of the lowest sintering temperature (associated with short heat treatment and applied pressure) in ………….. All the ceramics exhibit clean grain boundaries, except the ceramic processed by ……………. that shows some small particles at the surface of grain (white circle in Fig. 4f) which let suppose the presence of inter-granular precipitates. ……………. observations performed on the three ceramics confirm the presence of these intergranular precipitates with size less than 40 nm only in the case of the microwave treatment (blue arrows in Fig. 5f). These intergranular precipitates associated with high porosity could explain the low thermal conductivity observed for the ceramic sintered by microwaves. Some intra-granular precipitates are present in all ceramics processed by ………, ……….. and ……………….. (red arrows in Fig. 5).

Fig. 5. ………………….. of ceramics processed by:
………….. (a and b),
………….. (c and d)
………….. (e and f).

Using the software Image J, concentration of precipitates in the grain could be evaluated for the three different p-type ………….. ceramics. …….. ceramic has the highest concentration of precipitates, followed by ………………….. and ……… ceramic (Table 1). The composition of these precipitates from ……….. analysis in ……….. configuration and performed on big precipitates shows an increase of antimony and oxygen peaks intensity in comparison

with the same analysis performed in the matrix, close to the precipitates (Fig. 6).

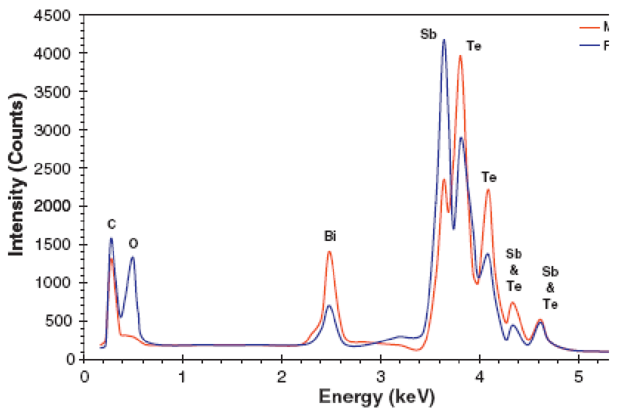


Fig. 6. ………………. of intragranular precipitates and matrix in the ……….. ceramic.

The composition of these precipitates is therefore believed to be some antimony oxide, Sb_2O_3 which corresponds to the most stable oxide in this type of materials [20]. The origin of oxygen in the initial powder could be attributed to some pollution occurring during mechanical alloying or during transport of packaging powders.

Thermoelectric performances of materials are always a deal between good electrical conductivity and low thermal conductivity. In the case of sample processed by ………, despite the good electrical properties (high electrical conductivity and power factor), the thermal conductivity remains high due to big grain size. As a consequence, the ZT value is low (ZT = 0.53). Electrical conductivities and power factor of both samples sintered by ……… and ………… techniques are weaker but the highest values of ZT in comparison with the ZT of ……… ceramic is due to lower thermal conductivity induced by smaller grain size for ……… ceramic or by the high porosity observed in microwaves ceramic. For similar compactness (……… and ……… techniques), the electrical conductivity is therefore linked to the grain size affecting the mobility which is consistent with the literature [21]. Scattering of electrons by grain boundaries and local defects seriously decrease the value of s. The presence or absence of antimony oxide precipitates seems to play also a key role in the thermal properties but their concentration are too low to impact considerably the value of thermal conductivity.

4. Conclusion

A p-type bismuth telluride powder synthesized by mechanical
alloying has been sintered by means of ……………………..
…………………………………………… …………………. Whatever the sintering technique and the differences of sintering parameters, no change in the …………………… is observed between the samples obtained by the ………… techniques. All ceramics contain more or less antimony oxide intra-granular precipitates and the microstructure (grain size) differs with the sintering technique. Electrical and thermal properties of the ceramics have been determined. The variations of thermoelectric properties between the ……………………… mainly come from the variations in charge carrier concentration. The highest value of ZT has been obtained for the ceramic processed by ………………… (ZT = 0.74) and by ………………… (ZT = 0.68). This result has been explained by the very low thermal conductivity of this ceramic due to high porosity in the …………………or by small grain size for the …………………, both samples keeping good Seebeck coefficient. We show that a low compactness (90%) is not detrimental for thermoelectric properties and that …………………………… techniques are a promising way to sinter thermoelectric materials providing an optimization of the composition of the alloy (amount of antimony) in order to get an optimized charge carrier concentration, this will allow to get higher ZT values.

In conclusion, future experiments will lie in optimizing, for the three different techniques, the charge carrier concentration by modifying the amount of antimony and the intra-granular precipitate

in the ceramics to get higher thermoelectric performances.

Acknowledgement
This work has been supported by the French National Agency (ANR) in the frame of its programme ‘‘Recherche

Technologique Nano-INNOV/RT’’ (THERMOINNOV project no. ANR-09-NIRT-007).

References

[1] F.J. DiSalvo, Science 285 (1999) 703–706.
[2] B.C. Sales, Science 295 (2002) 1248–1249.
[3] S.B. Riffat, X. Ma, Appl. Therm. Eng. 23 (2003) 913–935.
[4] L.E. Bell, Science 321 (2008) 1457–1461.
[5] G.J. Snyder, E.S. Toberer, Nat. Mater. 7 (2008) 105–114.
[6] W. Xie, X. Tang, Y. Yan, Q. Zhang, T.M. Tritt, Appl. Phys. Lett. 94 (2009) 102111.
[7] J. Yang, T. Aizawa, A. Yamamoto, T. Ohta, Mater. Chem. Phys. 70 (1) (2001) 90–94.
[8] H.P. Ha, T.H. Kim, D.B. Hyun, in: Proceedings ICT (International Conference on Thermoelectrics), 2001, pp. 117–120.
[9] M. Scheele, N. Oeschler, K. Meier, A. Kornowski, C. Klinke, H. Weller, Adv. Funct. Mater. 19 (2009) 3476–3483.
[10] H. Li, X.F. Tang, X.L. Su, Q.J. Zhang, Appl. Phys. Lett. 92 (2008) 202114.
[11] C. Wang, Z. Zhao, Scripta Mater. 61 (2009) 193.
[12] Z.A. Munir, U. Anselmi-Tamburini, M. Ohyanagi, J. Mater. Sci. 41 (2006) 763.
[13] M. Nygren, Z. Shen, Solid State Sci. 5 (2003) 125.
[14] D. Grossin, S. Rollin-Martinet, C. Estourne`s, F. Rossignol, E. Champion, C. Combes, C. Rey, G. Chevallier, C. Drouet, Acta Biomater. 6 (2010) 577.
[15] M. Oghbaei, O. Mirzaee, J. Alloy Compd. 494 (2010) 175–189.
[16] O. Kim-Hak, M. Soulier, P.-D. Skutnik, S. Saunier, J. Simon, Conférence Poudres et Matériaux Fritte´ s Saint-Etienne, France, May, 2011.
[17] D. Berardan, C. Byl, N. Dragoe, J. Am. Ceram. Soc. 93 (2010) 2352–2358.
[18] J. Jiang, L. chen, S. Bai, Q. Yao, Q. Wang, J. Cryst. Growth 277 (2005) 258–263.
[19] Y. Lan, A.J. Minnich, G. Chen, Z. Ren, Adv. Funct. Mater. 20 (2010) 357–376.
[20] S. Matsuo, M. Yonesto, H. Teshiro, K. Nakano, K. Takagi, J. Jpn. Inst. Met. 63 (1999) 1416–1422.
[21] H. Huang, W.-L. Luan, S.-T. Tu, Thin Solid Films 517 (2009) 3731–3734.

Final Control of Cermics and Glass

Le titre, l’abstract, mots clés, la fin de l’introduction, et la discussion peuvent être rédigés en français ou en anglais.
The abstract, key words, end of introduction and discussion are removed from the article published in ***Mater Sci Ceramics*** wish does not affect the understanding of the paper. You should reconstitute the papers as follow.

1- You should propose a new title of 6 words maximum
2- You should propose a new abstract of 6 lines maximum
3- You should propose a new key words 6 words maximum
4- You should propose a end of introduction of 5 lines maximum
5- You should propose a new discussion of 50 lines maximum

The non respect of the instructions will negatively impact the evaluation

Master Materials Engineering and Energy
***Module :* Ceramics and Glass**
Semestre 2
Pr. Saïd BENMOKHTAR

Title: ………………………………………………………… ……………………………….

N Anantharamulu[a], Radha Velchuri[a], T Sarojini[a], K Madhavi[b], G Prasad[b] & M Vithal[a]*

[a]Department of Chemistry, [b]Department of Physics, Osmania University, Hyderabad 500 007, India

Received 7 January 2008; accepted 4 August 2009

Abstract:
………
………
………
………
………

Keywords:
……

The discovery of NASICON [an abbreviation for Sodium (NA) super (S) ionic (I) conductor (CON)] increased the activity in the field of solid electrolytes considerably. Hong demonstrated that materials in the compositional range $Na_{1+x}Zr_2Si_xP_{3-x}O_{12}$ ($0 \leq x \leq 3$) crystallize in the NASICON structure, possessing a hexagonal framework structure and fast Na^+ transport comparable to that of β″-alumina[1,2]. The framework structure is a rigid, three-dimensional network of PO_4/SiO_4 (XO_4) tetrahedra sharing corners with ZrO_6 octahedra encapsulating the mobile sodium ion in the interconnected interstitial space. The infinite ribbons resulting from this linkage are connected together, perpendicular to the c-axis by PO_4 tetrahedra to form the NASICON framework. The Na^+ ions can occupy two positions, A_1 and A_2 in the conduction channels. The A_1 site (one per formula) is coordinated by a trigonal antiprism of oxygens and the A_2 site (three per formula) has distorted 8- fold coordination. A_1 and A_2 sites are located inside and between the ribbons respectively. It is observed that for x = 0 (corresponding to the composition $NaZr_2P_3O_{12}$), Na^+ ions completely occupy A_1 sites and A_2 sites are vacant. For compositions with $x > 0$, sodium ions start occupying the A_2 sites[3]. The site "A" can be substituted with ions such as H^+, NH^+, Cu^+ etc while the Zr site can be substituted with di, tri, tetra and penta valent ions. The NASICON family of materials has applications in ion selective electrodes, gas sensors, fuel cells and batteries[4-7]. Further, they are also used as mirror blanks in space technology[8], low thermal expansion ceramics[9], host for radioactive waste[10], catalyst supports[11] and in intercalation/deintercalation reactions[12,13]. Ceramic ionic (protonic) conductors are used as gas-impermeable membranes, for producing hydrogen by electrolysis of steam or other gases, and for the electrolytic removal of hydrogen from air and gas streams[14-18]. Presently, there is an intense

interest in finding a protonic conductor with high ionic conductivity due to its significance in a variety of analytical/electrochemical and potentiometric/ amperometric gas sensor applications[19]. The fully hydronium ion exchanged NASICON is known to be a fairly good protonic conductor[20].

....

....

Experimental Procedure

The composition $NaAlSb(PO_4)_3$ is prepared by sequential heating a stoichiometric mixture of NaH_2PO_4, Al_2O_3, Sb_2O_5 and $NH_4H_2PO_4$ (all AR grade chemicals) at 500˚C/5 h, 700˚C/5 h, 800˚C/10 h and finally 900˚C/16 h in an air with successive grinding at each stage as reported earlier[21]. $NaAlSb(PO_4)_3$ is found to be insoluble in HCl solution. About 2 g of $NaAlSb(PO_4)_3$ is taken in a round bottom flask and refluxed (a) once with 0.2 mol/L HCl solution for 6-8 h and (b) five times in fresh solutions of 0.5 mol/L HCl for 1 h. Each time, 10 mL of HCl per gram of powder is taken. After successive experiment, the solid is separated and filtrate is collected. The solid thus obtained is washed with distilled water and dried at 90˚C. This solid is designated as "solid A". The filtrate obtained at each stage is mixed and slowly evaporated to dryness. The solid obtained from this filtrate is named as "solid B".

Powder X-ray diffractograms are recorded at room temperature on Philips X'pert Analytical X-ray

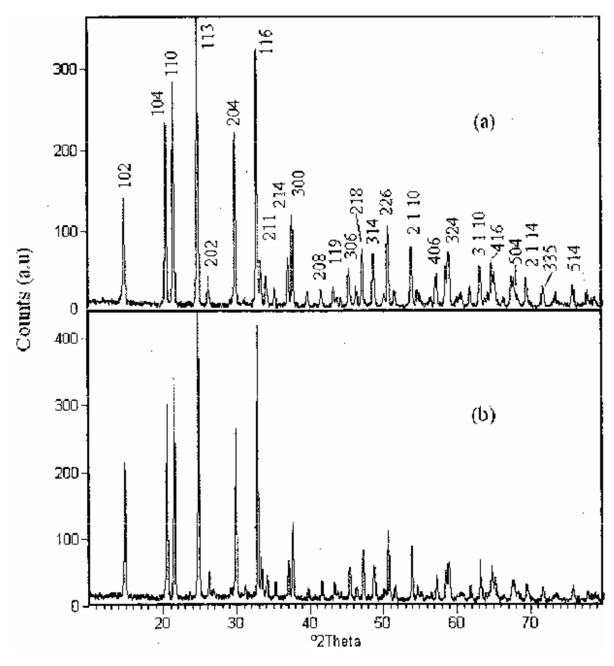


Fig. 1: Powder X ray diffraction pattern of (a) $NaAlSb(PO_4)_3$ and (b) solid A ($HAlSb(PO_4)_3$)

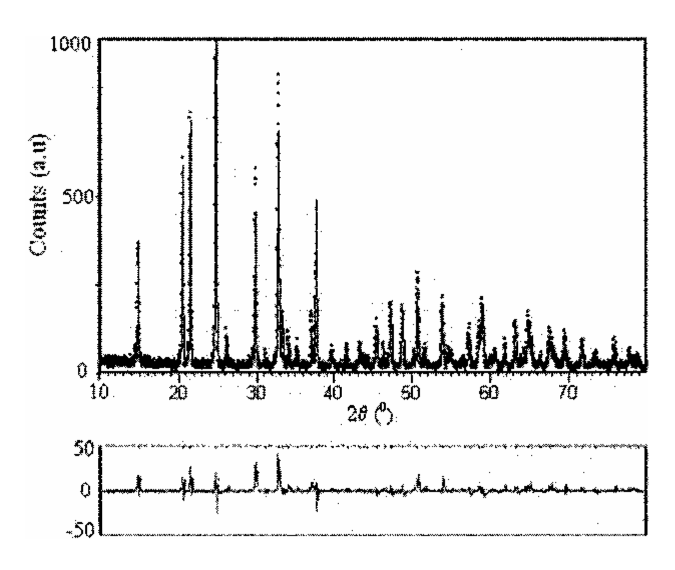


Fig. 2—Experimental (…), calculated (—) and difference profile of the XRD pattern of $NaAlSb(PO_4)_3$

diffractometer using Nickel filtered Cu-Kα radiation of wave length 1.5406 Å. The range of 2θ is 10° - 80° with increments of 0.003° and a counting time of 2 s. Rietveld refinement of the structures is performed using DBWS program[22]. Density of samples in the form of well sintered pellets is experimentally measured by Archimedes principle using xylene as an immersion liquid. Infrared spectra are recorded in the form of KBr pellets using JASCO FT/IR-5300 Spectrometer. TGA/DTA of powder samples was carried out on Mettler Toledo TGA/SDTA-851_e model in

nitrogen atmosphere in the temperature region 25-500ºC at the rate of 5ºC min^{-1}. The ^{31}P solid state MAS- NMR spectra are recorded with a Bruker DSX-300 MHz high resolution spectrometer operating at 121.49 MHz with an 8 kHz spinning speed. The samples are packed in a 4-mm Zirconia rotor. Pulses of 90º with 6.62 μs duration are employed with a recycle delay of 5 s between pulses. Both the spectra are recorded at room temperature. The chemical shift values are given with respect to an 85% H_3PO_4 solution.

The DC conductivities in the temperature range 30- 350°C are measured using a two-probe method on the sintered pellets coated with silver paint. A conventional sample holder and Keithley Electrometer 610C are used. The complex impedance of the sample between inert electrodes is measured using Auto Lab PGSTAT- 30 (excitation voltage: 30 V peak to peak sinusoidal voltage of varying frequency) low frequency impedance analyzer in the frequency range of 100 Hz to 1 MHz. The temperature range of impedance

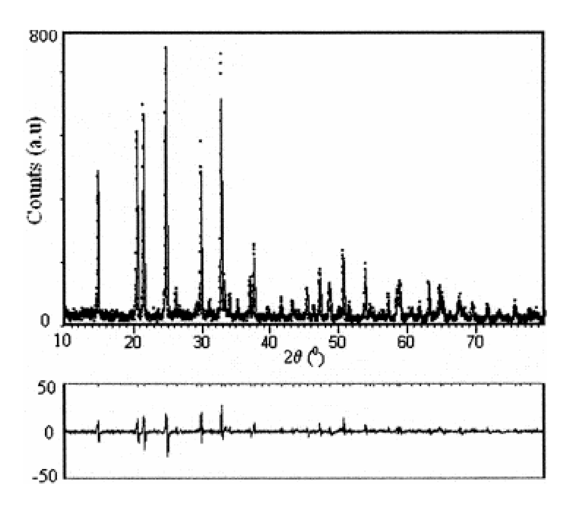


Fig. 3—Experimental (...), calculated (—) and difference profile of the XRD pattern of $HAlSb(PO_4)_3$

Table 1—Results of the Rietveld refinement of $NaAlSb(PO_4)_3$

Formula	$NaAlSb(PO_4)_3$
Profile fit	Pseudo-Voigt
Calculated density (g/cm^3)	3.50(1)
Experimental density (g/cm^3)	3.43(3)
Space group	$R\bar{3}c$
Lattice parameters	
a, *b*(Å)	8.292(4)
c (Å)	21.859(9)
α, β /°	90
γ /°	120
Volume (Å^3)	1301.52(3)
Coefficients for peak FWHM	
U	0.0000
V	0.0000
W	0.056(4)
Conventional Rietveld R-factors:	
R (expected)/ %	5.7
R (profile)/ %	7.3
R (weighted profile)/ %	6.9
R (Bragg)/ %	5.8

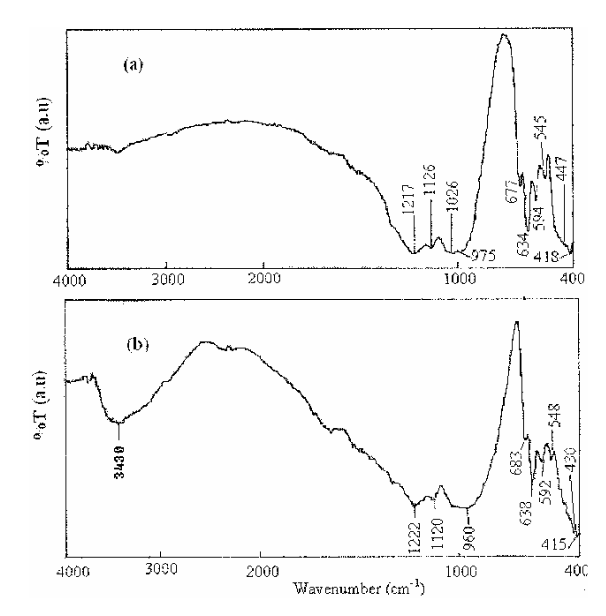


Fig. 4—IR spectra of (a) $NaAlSb(PO_4)_3$ and (b) $HAlSb(PO_4)_3$

Table 3: Results of the Rietveld refinement of $HAlSb(PO_4)_3$ Formula $HAlSb(PO_4)_3$

Profil fit ………………… ………	Pseudo voigt …………….
Calculated density (g/cm^3)	3.31(3)
(Experimental density (g/cm^3)	3.30(5)
Space group	R-3c
a, b (Å)	8.311(2)
c (Å)	21.862(5)
α, β /	90
γ / °	120
Volume	1307.67(2)
U	
V	
W	
Conventional Rietveld R-factors:	
R (expected)/ %	3.79
R (profile)/ %	7.68
R (weighted profile)/ %	8.47
R (Bragg)/ %	4.47

……………………………………………

……………………………………………

……………………………………………

……………………………………………

……………………………………………

……………………………………………

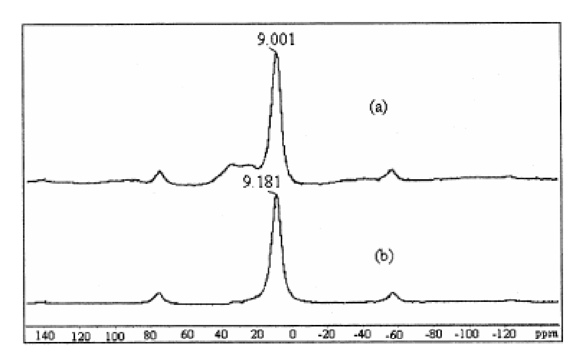
……………………………………………

Table 4—Occupancy, atomic fractional coordinates and isotropic displacement parameters of $HAlSb(PO_4)_3$

Atom	Site	Occ	*x*	*y*	*z*
H	6b	1.0	0.00000	0.00000	0.00000
Al	12c	0.5	0.00000	0.00000	0.1468(8
Sb	12c	0.5	0.00000	0.00000	0.1468(8
P	18e	1.0	0.2908(2)	0.00000	0.2500(1
O1	36f	1.0	0.1854(6)	0.9782(9)	0.1920(1
O2	36f	1.0	0.1889(6)	0.1635(8)	0.0852(8

Table 5—IR spectral data for $NaAlSb(PO_4)_3$ and $HAlSb(PO_4)_3$. (The band positions are in cm^{-1}; s = sharp, m = medium, w = weak

Compound	ν_3	ν_1	ν_4	ν_2
$NaAlSb(PO_4)_3$	1217m, 1126m, 1026w	975 m	677m, 634s	447w, 418m
$HAlSb(PO_4)_3$	1223m, 1120m	961 m	683m, 638s	430w, 415m



ig. 5—^{31}P-MAS NMR spectra of (a) $NaAlSb(PO_4)_3$ and (b) $HAlSb(PO_4)_3$

Conclusions

The compounds $NaAlSb(PO_4)_3$ and $HAlSb(PO_4)_3$ are prepared and characterized by powder XRD, IR and solid state ^{31}P MAS NMR techniques. Both the samples crystallize in hexagonal lattice of NASICON framework with the space group *R* 3 *c* . These samples show characteristic PO_4 vibrations in IR spectra. The solid-state ^{31}P-MAS NMR spectra of these samples suggest only one type of phosphorous in the hexagonal lattice. The impedance studies

Acknowledgements

The autors would like to thank the NMR centre Indian Institue of Science, Bangalore for providing the 31P-MAS NMR spectra and Director Defence Mettalurgical Research Laboratory (DMRL). Hyderabad for extending powder XRD facility.

References

1 Hong H Y P, *Mater Res Bull*, 11 (1976) 173.
2 Goodenough J B, Hong H Y P & Kafalas J A, *Mater Res Bull*, 11 (1976) 203.
3 Boilot J P, Colin G & Colomban P H, *J Solid State Chem*, 73 (1988) 160.
4 Mauvy F & Siebert E, Ahmad A, *J Euro Ceram Soc*, 19 (1999) 917.
5 Ling Wang & Kumar R V, *Solid State Ionics,* 158 (2003) 309.
6 Pasciak G, Prociow K, Mielcarek W, Gornicka B & Mazurek B, *J Eur Ceram Soc*, 21 (2001) 1867.
7 Chung S Y, Bloking J T & Chiang Y M, *Nature Mater*, 2 (2002) 123.
8 Dinesh Agrawal K & James Adair H, *J Am Ceram Soc*, 73 (1990) 2153.
9 Lightfoot P, Woodcock D A, Jorgensen J D & Short S, *Int J Inorg Mater*, 1 (1999) 53.
10 Balagopal S, Landro T, Zecevic S, Sutija D, Elangovan S, Khandkar A, *Sep Purif Technol*, 15 (1999) 231.
11 Youness Brik, Mohamed Kacimi, Francois Bozon-Verduraz & Mahfoud Ziyad, *Microporous Mater & Mesoporous Mater*, 43 (2001) 103.
12 Delmas C, Cherkaoui F, Nadiri A & Hagenmuller P, *Mater Res Bull*, 22 (1987) 631.
13 Kasthuri Rangan K & Gopalakrishnan J, *Inorg Chem*, 34 (1995) 1969.
14 Konishi S, Ohno H, Yoshida H & Naruse Y, *Nucl Technol*, 3
15 Konishi S, Ohno H, Yoshida H, Katsuta H & Naruse Y, *Int J Hydro Ener*, 11 (1986) 507.
16 Jensen J & Kleizt M, eds., in *Solid state protonic conductors I* (Odense University press, Odense, Denmark, 1982).
17 Goodenough J B, Jensen J & Kleizt M, eds, in *Solid state protonic conductors II* (Odense University press, Odense, Denmark, 1983).
18 Goodenough J B, Jensen J & Potier A, eds, in *Solid state protonic conductors III* (Odense University press, Odense, Denmark, 1984).
19 Maffei N & Kuriakose A K, *Sens Actuat B*, 98 (2004) 73.
20 Gulens J, Hildebrandt B W & Canaday J D, Kuriakose A K, Wheat T A, Ahmad A, *Solid State Ionics,* 35 (1989) 45.
21 Frank Berry J & Muga Vithal, *Polyhedron,* 14 (1995) 1113.
22 Abderrahim Aatiq, Rabia Hassine, My Rachid Tigha & Ismael Saadoune, *Powder Diffrac,* 20(1) (2005) 33.
23 Abderrahim Aatiq, My Rachid Tigha, Rabia Hassine & Ismael Saadoune, *Powder Diffract*, 21 (1) (2006) 45-51.
24 Nakamoto K, *Infrared and Raman Spectra of Inorganic and Coordination Compounds, Part I: Theory and Applications in Inorganic Chemistry* (Wiley, New York), 1997, p 159.
25 Barj M, Perthius H & Colombon P H, *Solid State Ionics*, 11 (1983) 157.
26 Mbandza A, Bordes E & Courtine P, *Mater Res Bull*, 20 (1985) 251.
27 Kazuo Nakamoto, *Infrared and Raman Spectra of Inorganic and Coordination Compounds* (Wiley, New York), 1978.
28 Nyquist R A & Kagel R O, *IR Spectra of Inorganic Compounds* (Academic Press, New York), 1971.
29 Sobha K C & Rao K J, *J Solid State Chem*, 121 (1996) 197.
30 Aatiq A, Menetrier M, El Jazouli A & Delmas C, *Solid State Ionics,* 150 (2002) 391.
31 Gulens J, Longhurst T H, Kuriakose A K & Canaday J D, *Solid State Ionics*, 28-30 (1988) 622.
32 Elliot S R, *Solid State Ionics*, 70-71 (1994) 27.
33 Losilla E R, Aranda M A G, Bruque S, Paris M A, Sanz J & West A R, *Chem Mater*, 10 (1998) 665.

UNIVERSITY HASSAN II OF CASABLANCA
FACULTY OF SCIENCES BEN M'SIK
DEPARTMENT OF CHEMISTRY

Master Materials Engineering and Energy
Module : **Ceramics and Glass**
Semestre 2
Pr. Saïd BENMOKHTAR

Spark plasma sintering and decomposition of the Y_3NbO_7:Eu phase

In: ***J Mater Sci***
Ceramics
Received: 26 July 2017
Accepted: 28 September 2017
By:
K. Y. Kim[1] , A. Veillere[1,2] , U-C. Chung[1] , V. Jubera[1,3] , and J.-M. Heintz[1,2],*
[1]CNRS, ICMCB, UPR 9048, 87 av Dr. Albert Schweitzer, 33600 Pessac, France
[2]Bordeaux INP, ICMCB, UPR 9048, 33600 Pessac, France
[3] University of Bordeaux, ICMCB, UPR 9048, 33600 Pessac, France

The abstract, key words, end of introduction and discussion are removed from the article published in ***Mater Sci Ceramics*** wish does not affect the understanding of the paper. You should reconstitute the papers as follow.

1- You should propose a new title of 6 words maximum
2- You should propose a new abstract of 6 lines maximum
3- You should propose a new key words 6 words maximum
4- You should propose a end of introduction of 5 lines maximum
5- You should propose a new discussion of 50 lines maximum

The non respect of the instructions will negatively impact the evaluation.

I/ Introduction

- Ceramics attract a lot of attention as alternative materials to glasses and single crystals in a number of application fields such as

(1) ……………

(2) ……………..,

(3) …..…………. and ………………….. [1–3].

- Considering optical materials, for which ………………. is required, ceramics can be used as

(1) ……………..,

(2) …………….., optical components and ……………….., [4–6].

- The first …………….. ceramics were obtained in the ……. [7]. The ………………. of these ceramics is directly related to ……………………. and ………………………..

- ……………….. and …………………… methods present the main advantage to strongly reduce the internal ……………., giving rise to relative densities of 99.9% [15, 16].

- Fast heating processes such as spark plasma sintering (SPS), ……………………….............

(PAS) or ……………………….......(PECS) are also giving high-density ceramics (C 99%) and in very short times [17–25].

- In our work, we propose to investigate the sintering of a new class of materials, i.e., rare earth niobates in order to study ………………………………….

What are rare earth elements? And why are they important?

…………………………………………………………………………………………………...

…………………………………………………………………………………………………...

Who many rare earth elements are in periodic table?

Figure 1 : Periodic table of the elements

Gives the limit of the atomic numbers of rare earth elements vary from Z_i to Z_j

Z_i = ……………., and Z_j= ………………..

Gives the electronic configuration of rare earth elements, then the electronic configuration of Eu^{3+}

………………………………………………………………………………………………

………………………………………………………………………………………………

II/ Materials and methods

High-purity-grade powders were used as starting materials studied in this work:

Rare earth oxides (…………..., Cerac, 99.99% and …………., Alfa Aesar, 99.99%),

Niobium (V) chloride (……………….Sigma-Aldrich, 99.998%),

Ethylene glycol (……………….., Sigma-Aldrich, 99%),

Citric acid (……………., Alfa Aesar, 99.5%) and methanol (……….., Sigma-Aldrich, [99.9%).

The complete description of the powder syntheses is given in ‘‘SPS sintering of powders obtained from **the solid-state route and from the sol–gel route‘‘.**

Equilibrium phase diagram

Below in **figure 2**, the binary system of Y_2O_3 and Nb_2O_5.

Give the phases present, their compositions in the phase diagram.
Gives the formula of stœchiometric compound with mole fraction $\chi = 0.50$.

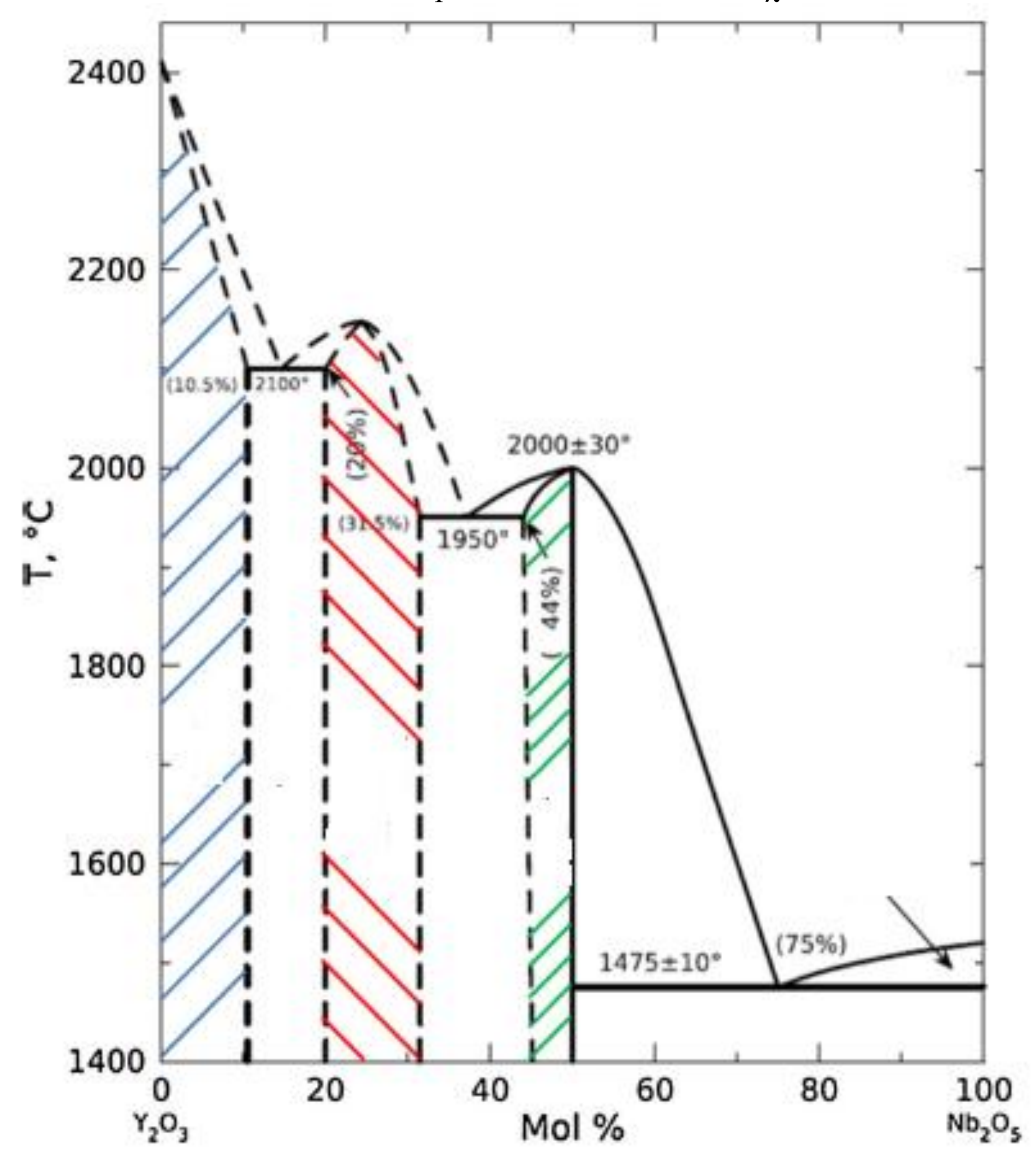


Figure 2: Y_2O_3–Nb_2O_5 equilibrium phase diagram.

II-a/ Section for the solid-state route

The synthesis of the material studied in this work, Eu^{3+}-doped Y_3NbO_7 niobate phase was first conducted using a solid-state reaction route (mixing and heat treatment of powders), starting ***from** ……………., ……………. **and** ……………. **oxide powders.***

Write a balanced chemical reaction correctly for the synthesis of compound

…………………………………………………………………………………………………

Gives the chemical composition chosen for the study ………………………..

The purity of final products was controlled after each step by X-Ray diffraction

At Room-temperature powder X-ray diffraction (XRD) patterns were collected on a PANalytical X'Pert MDP-PRO X-ray diffractometer with a Bragg–Brentano θ–2θ geometry using Cu $K_{\alpha 1,2}$ radiation (8\2θ\80°, with a step size of 0.02° and a counting time of 30 s)

To improve the synthesis, successive heat-treatment were performed at 1200°C, 1300°C, and 1400°C in air. But they were not sufficient to remove totally traces of impurities of oxides detected on the diffractograms.



What is the impurities of oxides detected?

…………………………………………………………………………………………………

…...……………………………………………………………………………………………

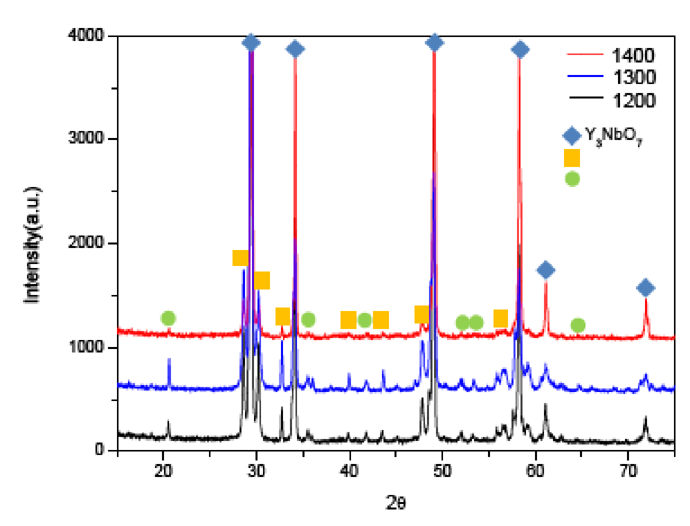


Figure 3: Evolution of X-ray patterns of powders obtained through solid state reaction

II-b/ SPS sintering of powders

Complete the schematic below of Spark plasma sintering

What mean the DC pulse sequence used for all the samples 12:2 (12 ON/2 OFF).

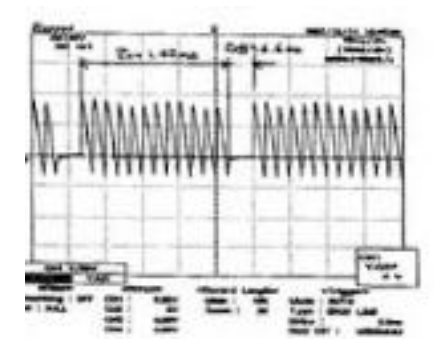


Figure 4: the DC pulse sequence

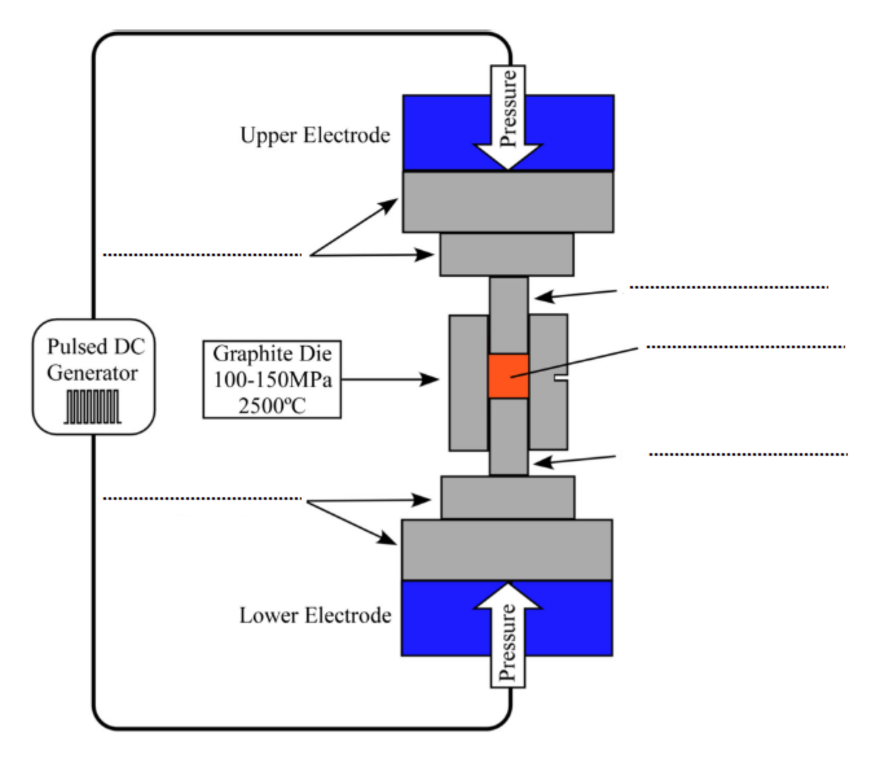


Figure 5: Schematic of the used SPS equipment (DR. SINTER LAB, Model SPS- 515S).

Optimization of the sintering conditions of the solid state powder

Explain the SPS sintering behavior of the calcined powder(solide state powder) mixture from the **Table 1 and Figure 5**

Table 1 Sintering conditions and final relative densities of solid state route powders sintered by SPS

SPS conditions	Relative density[a]
5 °C min^{-1}—1450 °C—20 min	$d_{rel} = 99.2\%$
5 °C min^{-1}—1520 °C—20 min	$d_{rel} = 99.5\%$
5 °C min^{-1}—1600 °C—20 min	$d_{rel} = 98.9\%$

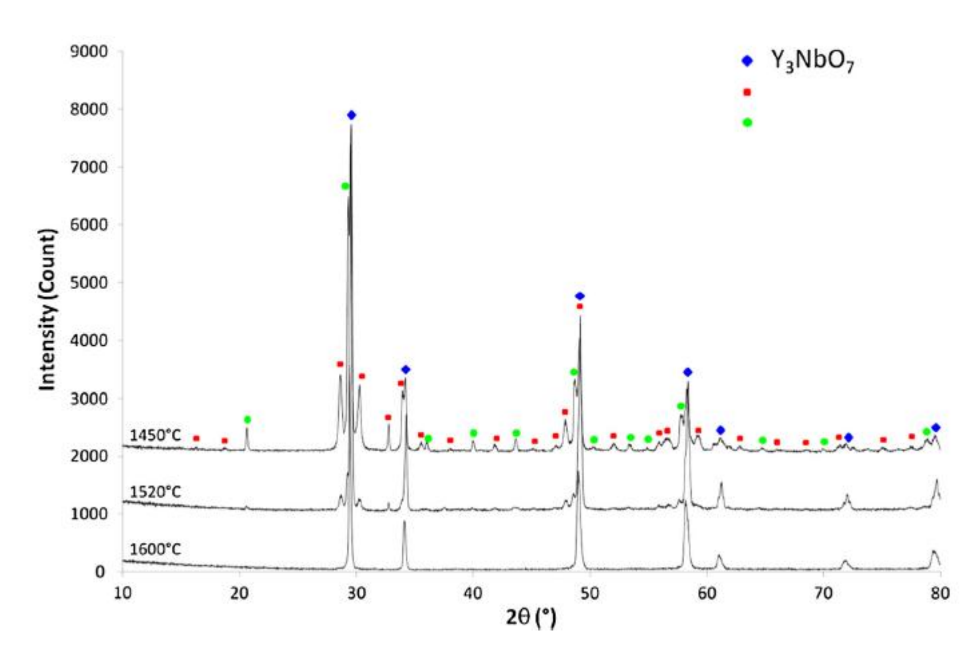


Figure 6: X-ray diffraction pattern of SPS sintered pellets as a function of the sintering temperature (1450, 1520 and 1600 °C).

II-c/ Section for the sol–gel route.

Describe the sol-gel method (Pechini route) for synthesis of Eu^{3+}-doped Y_3NbO_7 niobate phase

…………………………………………………………………………………………………

…………………………………………………………………………………………………

Why we use concentrated acid nitric?

…………………………………………………………………………………………………

Why we use methanol?

…………………………………………………………………………………………………

Why we added ethylene glycol to the solution

…………………………………………………………………………………………………

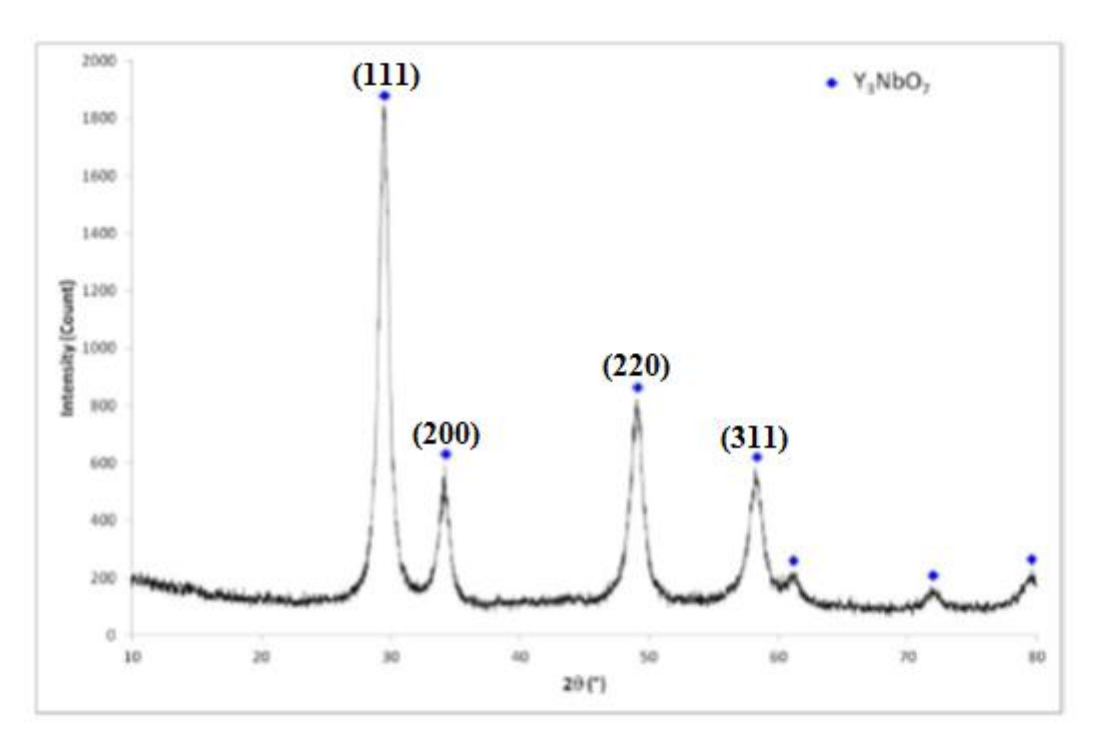


Figure 7: X-ray pattern of sol-gel powder heat treated at 700°C under O_2

The Pechini (sol-gel) synthesis seems to be the best method to prepare Eu^{3+} doped Y_3NbO_7 powder.

X-Ray diffraction patterns are all consistent with the so-called defect-fluorite family, cubic type structure **(JPDS N° 01-074-6421)** compatible with the $Fm\overline{3}m$ symmetry group.

Determine the lattice parameter of the unit cell of the compound synthesis

…………………………………………………………………………………………………

…...……………………………………………………………………………………………

Gives the Scherrer's equation to calculate he average crystallite size of powder (9nm)

…...……………………………………………………………………………………………

Optimization of the sintering conditions of the sol–gel powder

Explain the SPS sintering behavior of the calcined powder (sol–gel powder) mixture from the Table 2 and Figure 8

Table 2: Sintering conditions and final relative densities of sol– gel powders sintered by SPS

SPS conditions	Relative density
5 °C min^{-1}—1600 °C—10 min	d_{rel} = 98.7%
5 °C min^{-1}—1600 °C—20 min	d_{rel} = 98.4%
5 °C min^{-1}—1600 °C—40 min	d_{rel} = 97.8%
5 °C min^{-1}—1600 °C—120 min	d_{rel} = 95.9%
5 °C min^{-1}—1600 °C—20 min	d_{rel} = 98.4%
10 °C min^{-1}—1600 °C—20 min	d_{rel} = 98.9%
50 °C min^{-1}—1600 °C—20 min	d_{rel} ~ 90%

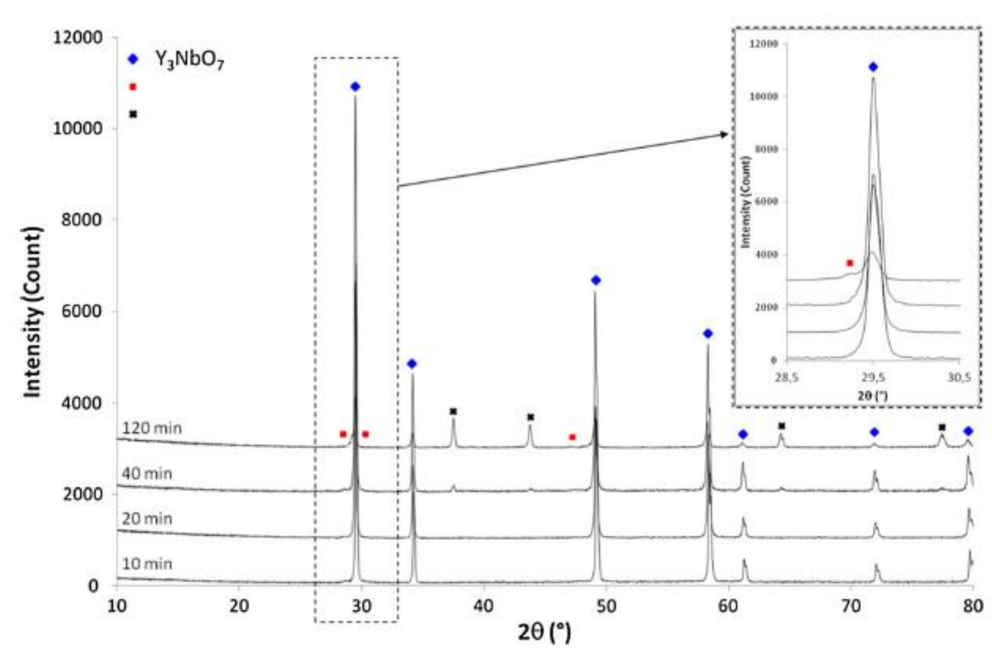


Figure 8: X-ray diffraction patterns of SPS pellets (sol–gel powder), as a function of sintering time at 1600 °C (10, 20, 40 and 120 min).

SPS relative densities remain lower than 99% for all samples and these values seem to decrease when sintering time increases. ***Explain the evolution of XRD and densities***.

…………………………………………………………………………………………...

…………………………………………………………………………………………...

…………………………………………………………………………………………...

From Table 2 and Figure 9, explain the effect of the role of the heating rate investigated. Sintering results are given in **Table** 2, and the microstructure of fractured pellets is presented in Fig. 9

Figure 9 :SEM micrographs of fractured SPS pellets (sol–gel powder), sintered at 1600 °C during 20 min as a function of SPS heating ramp a 5 °C min^{-1}, b 10 °C min^{-1}, c 50 °C min^{-1}.

…………………………………………………………………………………………...

…………………………………………………………………………………………...

…………………………………………………………………………………………...

…………………………………………………………………………………………...

…………………………………………………………………………………………...

II-d/ Scanning Electron Microscopy (SEM)

The morphology of the as-prepared and heat-treated powders, as well as the microstructure of the densified pellets, was observed by scanning electron microscopy (TESCAN Vega II SBH SEM).

What is Scanning Electron Microscopy (SEM)

……………………………………………………………………………………………...



Figure 10 :Instrument of SEM

What are the two main types of electron microscopes

……………………………………………………………………………………………...

……………………………………………………………………………………………...

Give a title to a figure, and explain

……………………………………………………………………………………………...

……………………………………………………………………………………………...

……………………………………………………………………………………………...

……………………………………………………………………………………………...

UNIVERSITY HASSAN II OF CASABLANCA *UNIVERSITY ANNUAL 2018-2019*
FACULTY OF SCIENCES BEN M'SIK
DEPARTMENT OF CHEMISTRY

Master Materials Engineering and Energy
Module : **Ceramics and Glass**
Semestre 2
Pr. Saïd BENMOKHTAR

1) Décrire les structures ci dessous, (Nommer les atomes, feuillet, ...)
2) D'après la théorie de L. PAULING en 1932, l'ionicité notée *I* d'une liaison entre deux atomes A et B qui mesure le pourcentage ionique de la liaison A-B s'exprime par une relation de la forme : $I_{A-B} = 100 \times \left\{ 1 - e^{-\frac{(\chi_A - \chi_B)^2}{4}} \right\}$, Type de liaison chimique qui existe dans les couches.
on donne : $\chi_{Si} = 1,5$, $\chi_{Al} = 1,8$, $\chi_O = 3,5$,
3) En déduire la formule chimique de cette argile.
4) De quel type d'argile s'agit-il ?

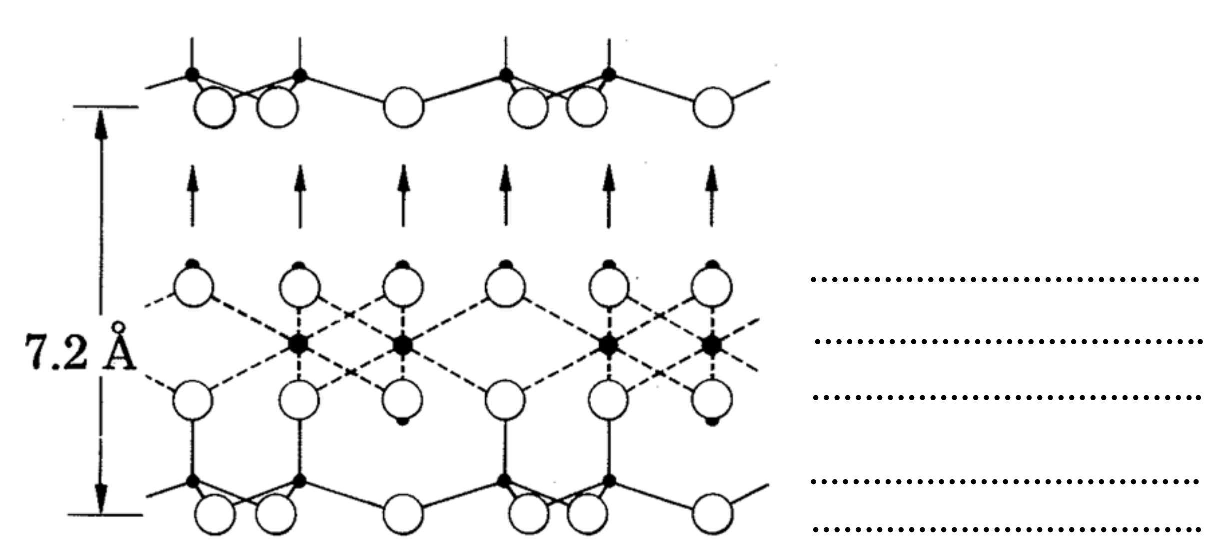
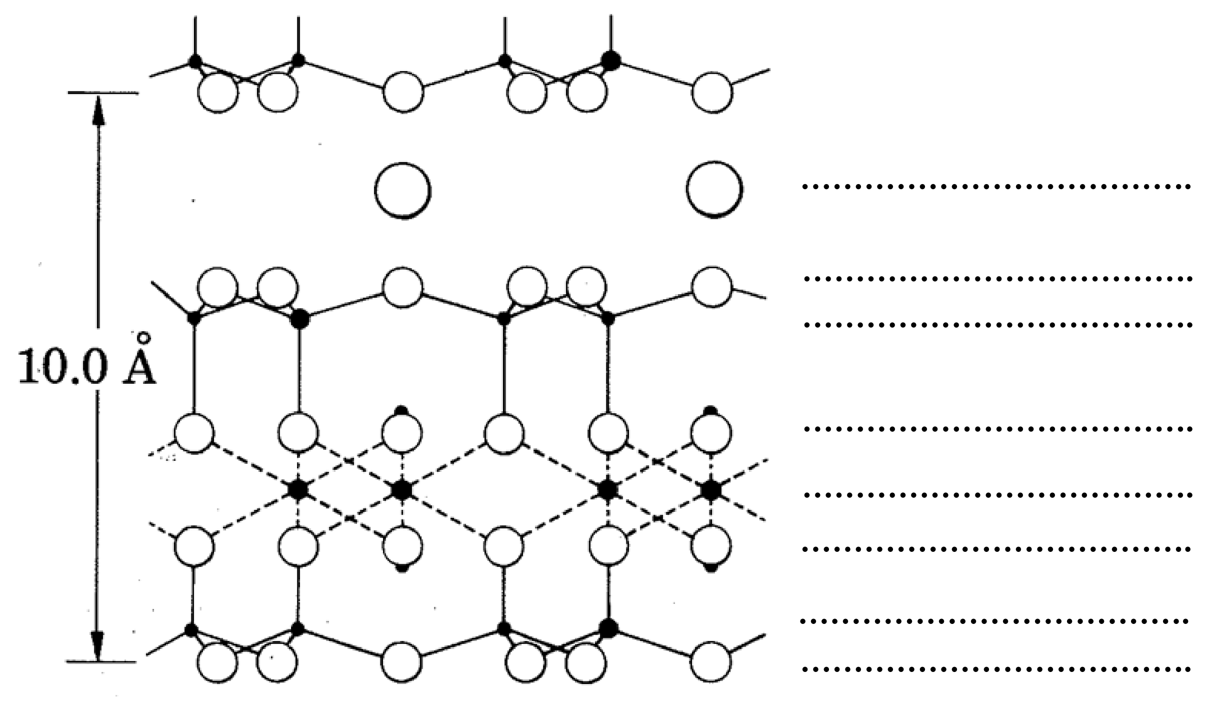


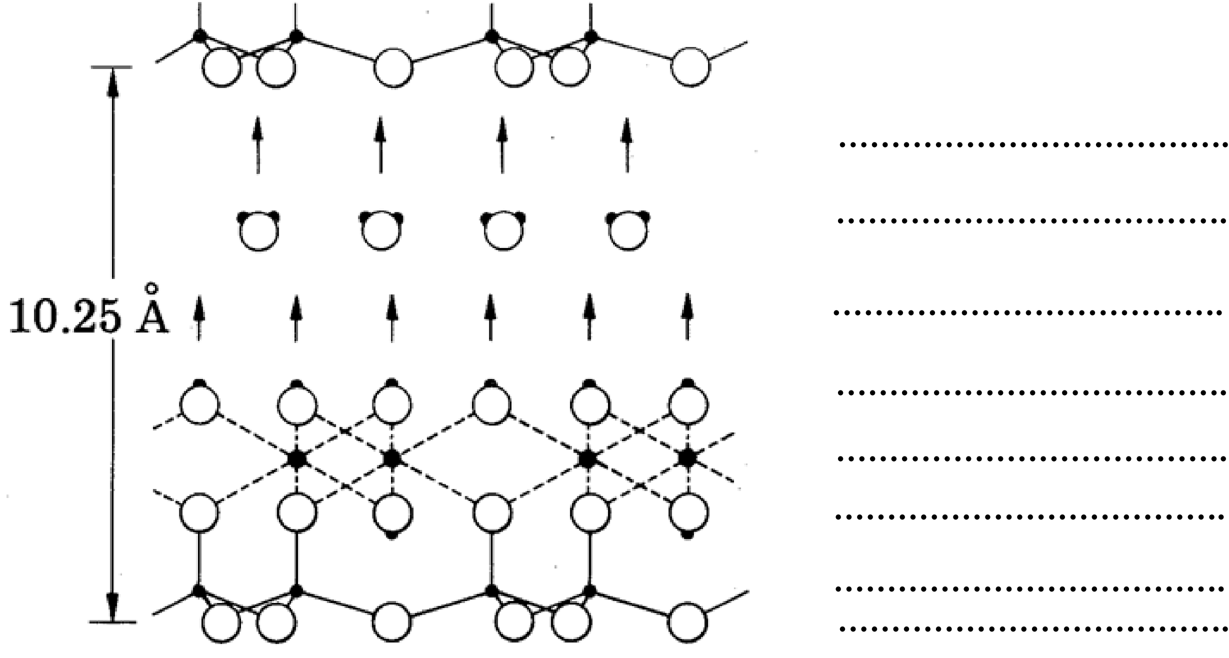
Figure 1 ***: structure cristalline d'une argile type 1/1***

Formule chimique de l'argile A: ……………………………………………………………..



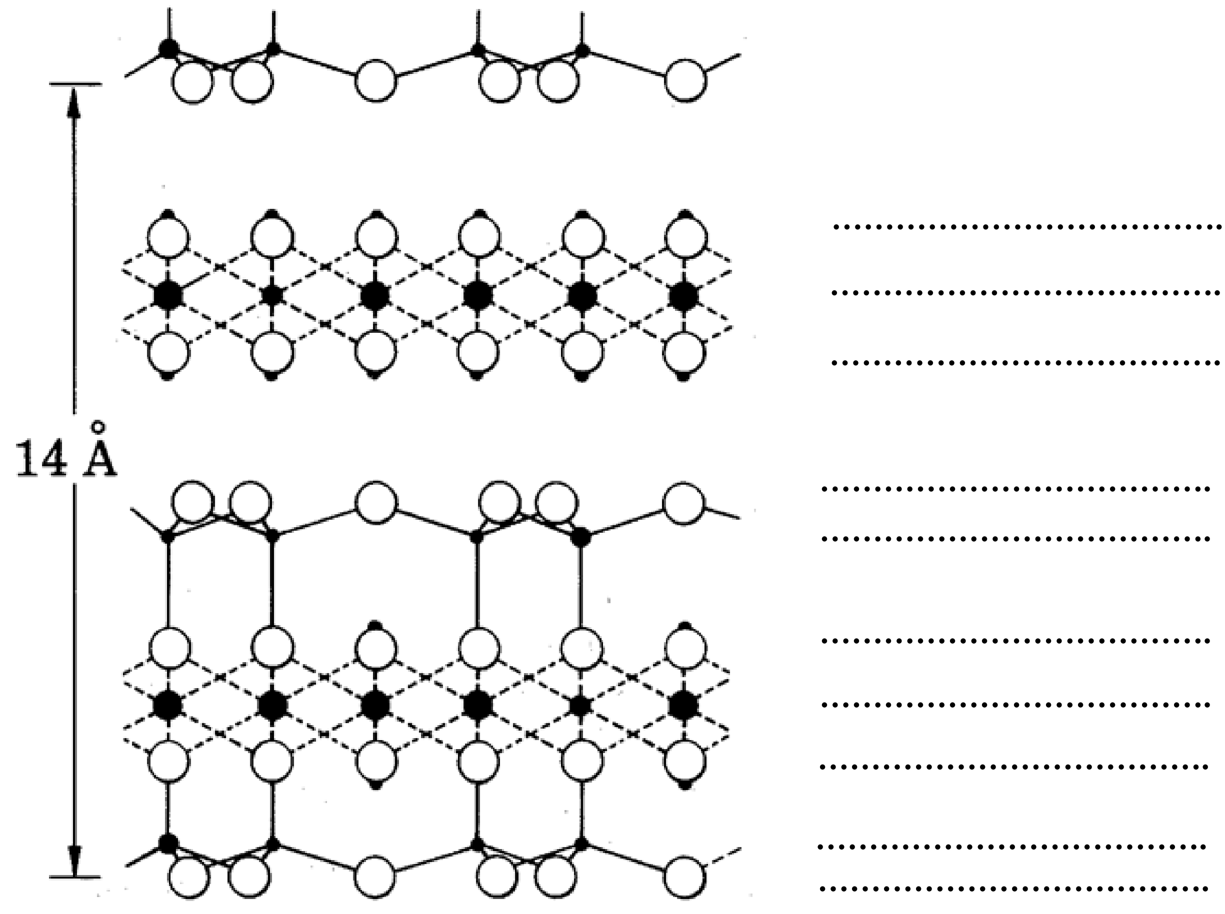
<u>Figure 2</u> : structure cristalline d'une argile 2/1

Formule chimique de l'argile B: ……………………………………………………………..



<u>Figure 3</u> : structure cristalline d'une argile 2/1

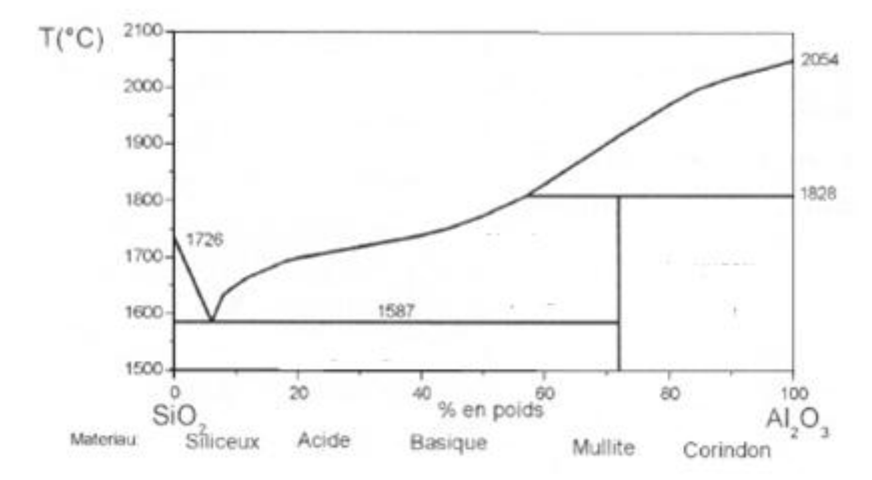
Formule chimique de l'argile C:………………………………………………………………..



<u>Figure 4</u> : structure cristalline d'une argile 2/1/1

Formule chimique de l'argile D:…………………………………………………………..

B- Compléter le diagramme binaire : SiO_2-Al_2O_3



C- L'halloysite est une phase principale constitutive des kaolins: elle ne diffère de la kaolinite que par la quantité d'eau zéolitique plus élevée qu'elle renferme et sa formule chimique

1) Expliquer c'est quoi une eau zéolitique
2) Decrire la morphologie de l'halloysite

UNIVERSITY HASSAN II OF CASABLANCA *UNIVERSITY ANNUAL 2018-2019*
FACULTY OF SCIENCES BEN M'SIK
DEPARTMENT OF CHEMISTRY
Master Materials Engineering and Energy
Module : **Ceramics and Glass**
Semestre 2
Saïd BENMOKHTAR

1) Traditional ceramics comprise three main components, clay, quartz and feldspar. What is the role of the feldspar component?

a- To bind the refractory components together

b- To improve the workability of the system prior to firing

c- To form Mullite on firing

d- To lower the cost

e- To control the colour of the product.

1. The word ‘ceramic’ meant for

(a) soft material	(b) hard material	(c) burnt material	(d) dry material

2. Not a characteristic property of ceramic material

(a) high temperature stability	(b) high mechanical strength
(c) low elongation	(d) low hardness

3. Major ingredients of traditional ceramics

(a) silica	(b) clay	(c) feldspar	(d) all

4. Not a major contributor of engineering ceramics

(a) SiC	(b) SiO_2	(c) Si_3N_4	(d) Al_2O_3

5. The following ceramic product is mostly used as pigment in paints

(a) TiO_2	(b) SiO_2	(c) UO_2	(d) ZrO_2

6. Most commercial glasses consist of

(a) lime	(b) soda	(c) silica	(d) all

7. Hot isostatic pressing is not a viable option if the chief criterion is

(a) strength without grain growth	(b) lost cost	(c) zero porosity	(d) processing refractory ceramics

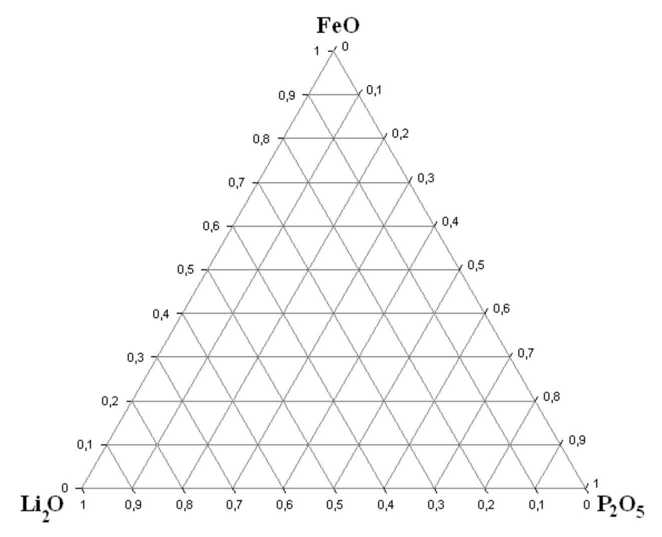
8. During sintering densification is not due to

(a) atomic diffusion	(b) surface diffusion	(c) bulk diffusion	(d) grain growth

UNIVERSITY HASSAN II OF CASABLANCA *UNIVERSITY ANNUAL 2018-2019*
FACULTY OF SCIENCES BEN M'SIK
DEPARTMENT OF CHEMISTRY
Master Materials Engineering and Energy
***Module :* Ceramics and Glass**
Semestre 2
Saïd BENMOKHTAR

1- Synthèse:

Le matériau $LiFePO_4$ peut être synthétisé par méthode hydrothermale, à partir des précurseurs suivant : $FeSO_4 \cdot 7H_2O$ (98% Fisher), H_3PO_4 (85 wt.% solution Fisher), LiOH (98% Aldrich).
1) Décrire cette méthode.
2) Ecrire la réaction de synthèse de $LiFePO_4$ par méthode hydrothermale.
3) Représenter dans le diagramme ternaire Li_2O-FeO-P_2O_5 (figure 1), les compositions suivantes : $LiFePO_4$ et $LiFe_4(PO_4)_3$



2- Caractérisation de la céramique

2-a) Quelles techniques peut-on utiliser pour connaître :
- le degré d'oxydation et la nature du site occupé par les ions du Fer.
- le nombre du site du Phosphore et la nature du site.

On donne sur la figure 2 le diffractogramme X de poudre de la céramique $LiFePO_4$.

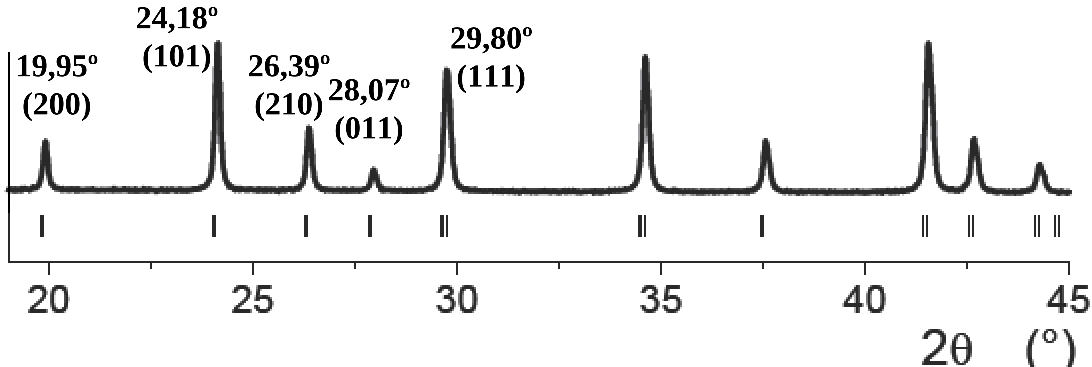


Figure 2: Diffractogramme X du matériau $LiFePO_4$ (anticathode de Co, λ_{Co}=1,79Å)

2-b) Rappeler l'expression donnant les distances inter-réticulaires d_{hkl} dans le système orthorhombique.
2-c) En déduire les paramètres de maille a, b et c dans ce système.
2-d) Déterminer le nombre de motif par maille.
On donne : Masse molaire : Li : 6,94 ; Fe: 55,84 , P: 30,97, O :16
densité : 3,59, N=6,02.10^{23} mol^{-1}

3- Calcul de densité

Mesure de la densité apparente (géométrique) du corps fritté (compacte) de $LiFePO_4$
Cette détermination va être faite par calcul du volume de l'échantillon en supposant qu'il a une forme cylindrique parfait.
Soit une pastille de masse m = (1,3562 ± 0,0001) g de forme cylindrique de hauteur h = 3 mm et de rayon r = 5 mm.
3-a) Calculer le volume de la pastille V et la densité apparente ρ = masse/volume
3-b) Calculer le pourcentage de porosité (%) à partir de la formule suivante :

$$\% \, porosité = \frac{(\rho_{théorique} - \rho_{mesuré})}{\rho_{théorique}} \times 100$$

Frittage conventionnel

L'obtention de matériaux massifs par frittage de poudres est une étape primordiale en vue de la maîtrise des propriétés finales du matériau. En effet, l'étape de consolidation du compact pulvérulent par traitement thermique (frittage) va conditionner les propriétés microstructurales des frittés (porosité, taille de grains…).

- Expliquer un frittage naturel
- Frittage sous charge
- Frittage "Flash" (Spark Plasma Sintering (SPS))

UNIVERSITY HASSAN II OF CASABLANCA *UNIVERSITY ANNUAL 2018-2019*
FACULTY OF SCIENCES BEN M'SIK
DEPARTMENT OF CHEMISTRY
Master Materials Engineering and Energy
Module : **Ceramics and Glass**
Semestre 2
Saïd BENMOKHTAR

1) Translate the text
In our age cement is the most important binder in construction. Its two main types are: portland cement (a silicate binder) and alumina cement (aluminate cement). The hydraulic hardening is provided in portland cement by calcium silicates, in alumina cement by calcium aluminates.
....
....
....
....

2) What is Cement?

....
....

3) How can I determine the composition of clinker?

....
....
....

4) Gives the formula of the four main components of clinker

....
....
....
....
....

5) To make the formulas of cement minerals, compounds, and reactions shorter and easier to read, it is traditional to use a shorthand notation that leaves out the oxygen.

Complete the table:

Oxide form							
Notation	C	S	A	S	H	M	N

6) Thermochemistry of Clinker

The raw materials entered into the kiln are taken at room temperature. Inside the kiln, the temperature continues to rise and when it reaches its peak, clinker is produced by rapid cooling.

Though the reaction stages often overlap, they can be expressed in a sharply-defined sequence as follows:

1) **Write** all chemical **reaction** correctly of synthesis of cement.

a) 65-125°C: Free water evaporates: latent heat must be supplied.

....

b) 400-650°C: Clays decompose endothermically, and alkalis react with the kiln atmosphere to form liquid sulfates.

....

....

c) 500-650°C: Dolomite decomposes endothermically.

....

....

d) 650-900°C: Calcium carbonate reacts endothermically with silica to form "incipient belite".

....

....

e) 700-900°C: Calcium carbonate reacts endothermically with alumina and iron oxide to form incipient aluminate and ferrite.

....

....

f) 900-1050°C: When all available silica, alumina and iron oxide have reacted, the remaining calcium carbonate decomposes endothermically to calcium oxide.

....

....

g) 1300-1425°C: Aluminate, ferrite and part of the belite melt endothermically, and belite react with calcium oxide to form alite.

....

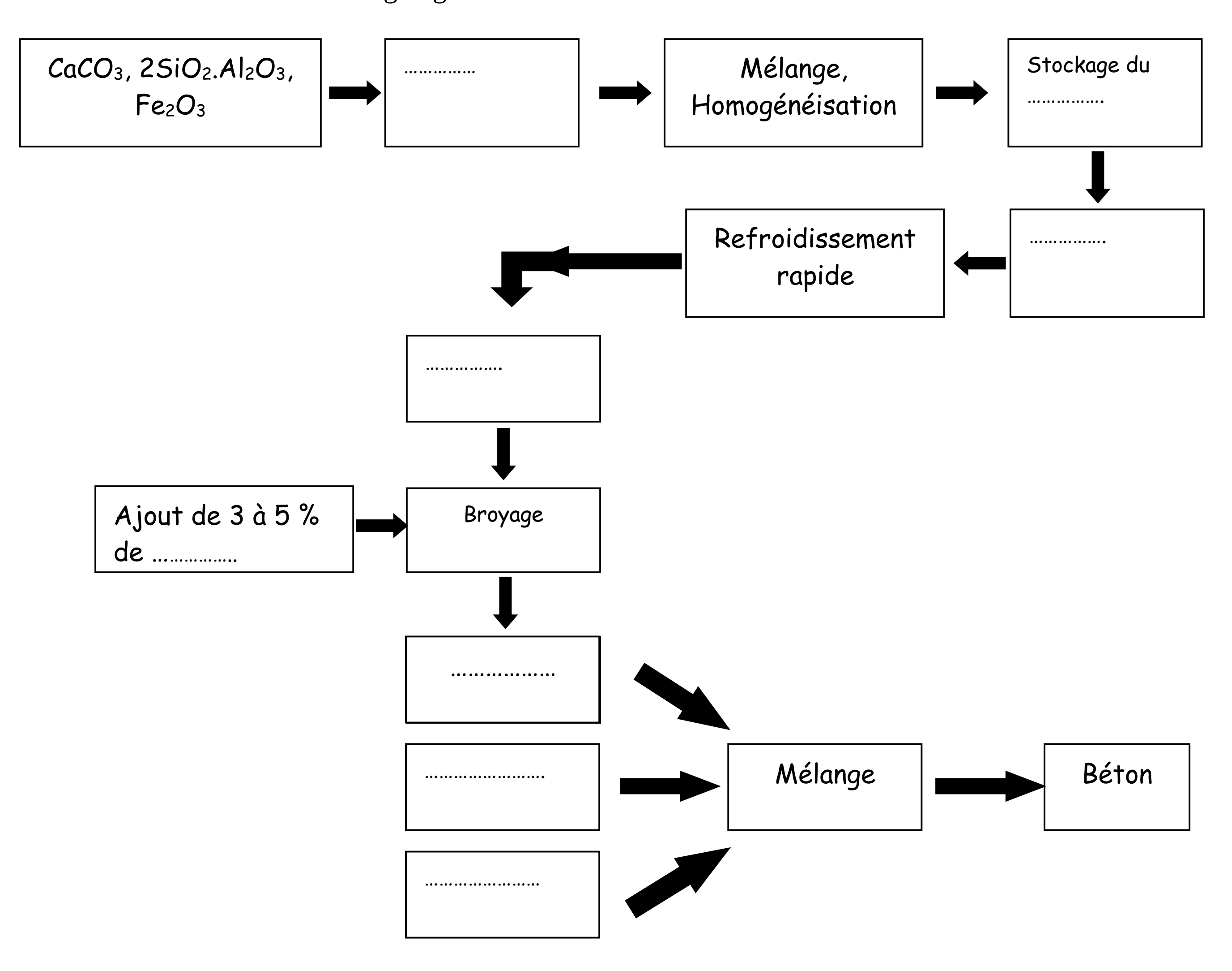
....

UNIVERSITY HASSAN II OF CASABLANCA
FACULTY OF SCIENCES BEN M'SIK
DEPARTMENT OF CHEMISTRY
UNIVERSITY ANNUAL 2018-2019

Master Materials Engineering and Energy
Module : **Ceramics and Glass**
Semestre 2
Saïd BENMOKHTAR

B) - 1) On propose un organigramme incomplet de la fabrication du ciment et du béton. Compléter cet organigramme à l'aide de certains mots de la liste suivante :
adjuvant- broyage- ciment- colorant– clinker– eau- fagot- four- gypse– laitier- pouzzolane- granulats- acier - chlorure de sodium- cru- cuit

Organigramme de fabrication du ciment



2) Lors de la formation du clinker, les oxydes principaux apportés par les matières premières se combinent entre eux pour former d'autres minéraux :
Ecrire les équations chimiques qui ont lieu durant la cuisson :

3-a) Entre 0 à 550°C

....

....

....

3-b) Entre 600 et 1100°C

....

....

....

3-c) Entre 1200 et 1450°C (Clinkérisation)

....

....

....

....

UNIVERSITY HASSAN II OF CASABLANCA *UNIVERSITY ANNUAL 2018-2019*
FACULTY OF SCIENCES BEN M'SIK
DEPARTMENT OF CHEMISTRY
Master Materials Engineering and Energy
Module : **Ceramics and Glass**
Semestre 2
Saïd BENMOKHTAR

It's important to understand what the text is about. Then you have to write the correct word(s) to complete a text.

……………… are electromagnetic radiation, whose wavelengths lie in the range of 1mm to 1m (frequency range of 0.3–300 GHz). Only narrow frequency windows centered at 900MHz and 2.45 GHz are allowed for ……………… heating purposes. Many ……………… preparations reported in the literature have been done on the laboratory scale of only a few grams. These syntheses have all been made with the use of domestic type of ……………… ovens which operates at 2.45 GHz with a maximum output power of 1 kW. Nowadays, large industrial types of ……………… furnaces are manufactured for the production of many chemicals in larger quantities.

EXERCICE II:

It's important to understand what the text is about. Then list the materials used in this synthesis method. And gives the main topics of this synthesis.

$BaK_4U_3O_{12}$ were grown out of molten potassium carbonate. 1/3 mmol of U_3O_8 (Strem Chemicals, 99.8%), 1 mmol of NiO (Alfa, 99.998%), 3mmol of $BaCO_3$ (Alfa, 99.95%) and 10 g of K_2CO_3 (Alfa, A.C.S. grade, 99%) flux were loaded into an alumina crucible loosely covered with an alumina lid. The charges were placed into a tube furnace and heated to 1050 °C at 600 °C/h. The furnace was held at the target reaction temperature for 24 h, after which time it was cooled to 850 °C at a rate of 20 °C/h, and subsequently cooled to room temperature by shutting off the furnace. Orange octahedral blocks of $BaK_4U_3O_{12}$ were isolated from the flux by dissolving the flux with water and collecting the $BaK_4U_3O_{12}$ by vacuum filtration.

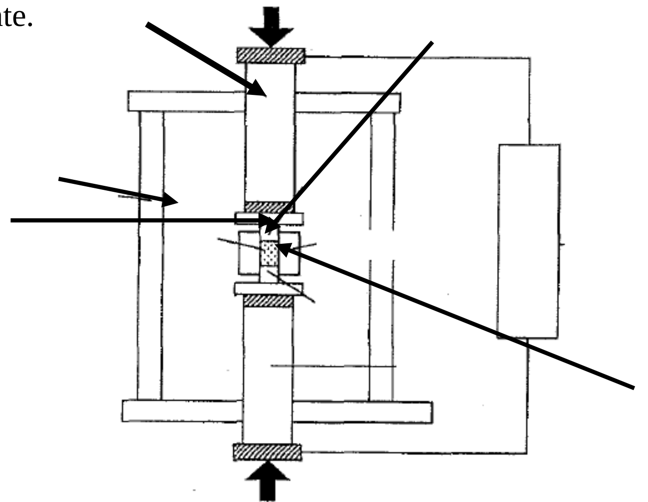
UNIVERSITY HASSAN II OF CASABLANCA
FACULTY OF SCIENCES BEN M'SIK
DEPARTMENT OF CHEMISTRY

UNIVERSITY ANNUAL 2018-2019

Master Materials Engineering and Energy
Module : **Ceramics and Glass**
Semestre 2
Pr. Saïd BENMOKHTAR

Control (1)

1) Qu’est-ce qu’une céramique thermomécanique ?
2) Donner un exemple de céramique thermomécanique.
3) Citer les trois étapes de l’élaboration d’une céramique.
4) Décrire brièvement les avantages de la technique de Frittage SPS
5) Compléter la figure suivante.

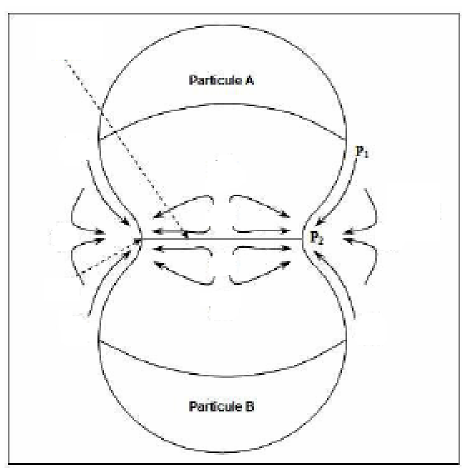


UNIVERSITY HASSAN II OF CASABLANCA *UNIVERSITY ANNUAL 2018-2019*
FACULTY OF SCIENCES BEN M'SIK
DEPARTMENT OF CHEMISTRY

Master Materials Engineering and Energy
Module : **Ceramics and Glass**
Semestre 2
Pr. Saïd BENMOKHTAR

Control (2)

1) Qu'est-ce qu'une céramique thermomécanique ?
2) Donner un exemple de céramique thermomécanique.
3) Citer les trois étapes de l'élaboration d'une céramique.
4) Expliquer à l'aide d'un schéma le mécanisme de formation du cou par la technique spark plasma
5) Expliquer ce mécanisme de diffusion lors du frittage par spark plasma



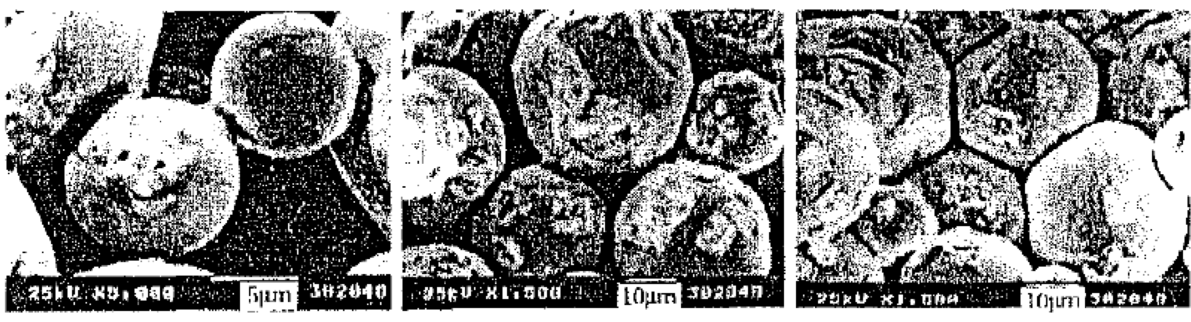
UNIVERSITY HASSAN II OF CASABLANCA
FACULTY OF SCIENCES BEN M'SIK
DEPARTMENT OF CHEMISTRY

UNIVERSITY ANNUAL 2018-2019

Master Materials Engineering and Energy
Module : **Ceramics and Glass**
Semestre 2
Pr. Saïd BENMOKHTAR

Control (3)

1) Les céramiques peuvent-être mises en forme par dépôt. Citez une des techniques et donnez une application.
2) Définir la porosité, et donner l'ordre de grandeur de la largeur des micropores, mésopores et des macropores
3) Nommer chaque étape du processus de frittage par Spark plasma.



UNIVERSITY HASSAN II OF CASABLANCA *UNIVERSITY ANNUAL 2018-2019*
FACULTY OF SCIENCES BEN M'SIK
DEPARTMENT OF CHEMISTRY

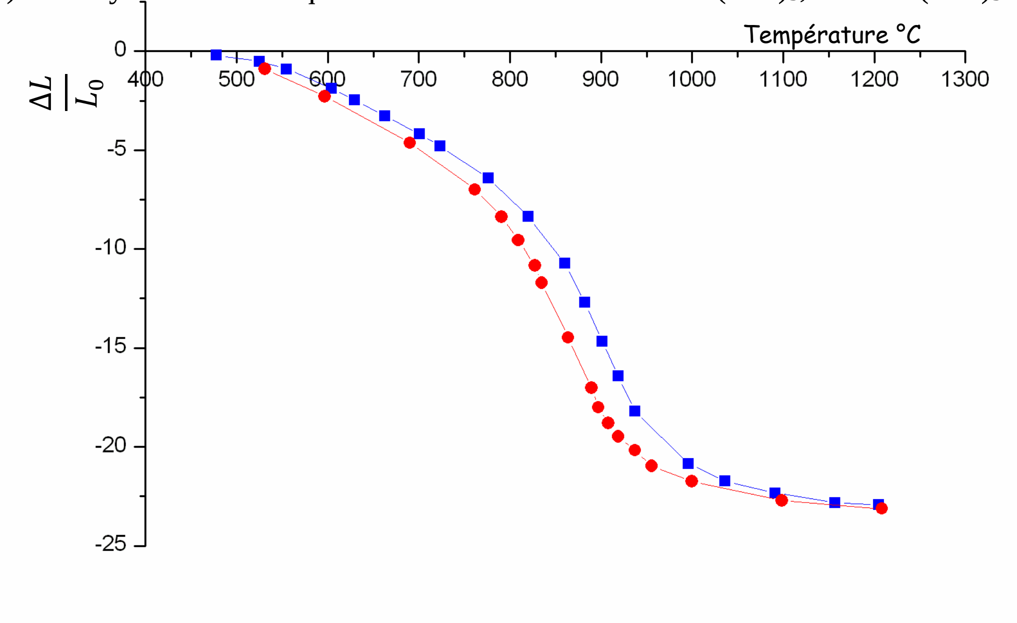
Master Materials Engineering and Energy
Module : **Ceramics and Glass**
Semestre 2
Pr. Saïd BENMOKHTAR

Control (4)

1) Les céramiques peuvent-être mises en forme par dépôt. Citez une des techniques et donnez une application.
2) Définir la porosité, et donner l'ordre de grandeur de la largeur des micropores, mésopores et des macropores.
Quelles informations apportent la dilatomètrie ?
3) Pour l'étude par dilatomètrie on utilise la formule ci-dessous pour exprimer l'état de densification instantané pendant le frittage
3-a) Donner la signification de chaque terme.
3-b) Démontrez cette formule (supposition retrait isotrope)

$$\frac{dD}{dt}\left(\frac{1}{D}\right) = -\frac{3}{L} \times \frac{dL}{dt}$$

4) L'analyse dilatométrique des deux échantillons $NaZr_2(PO_4)_3$, et $KZr_2(PO_4)_3$



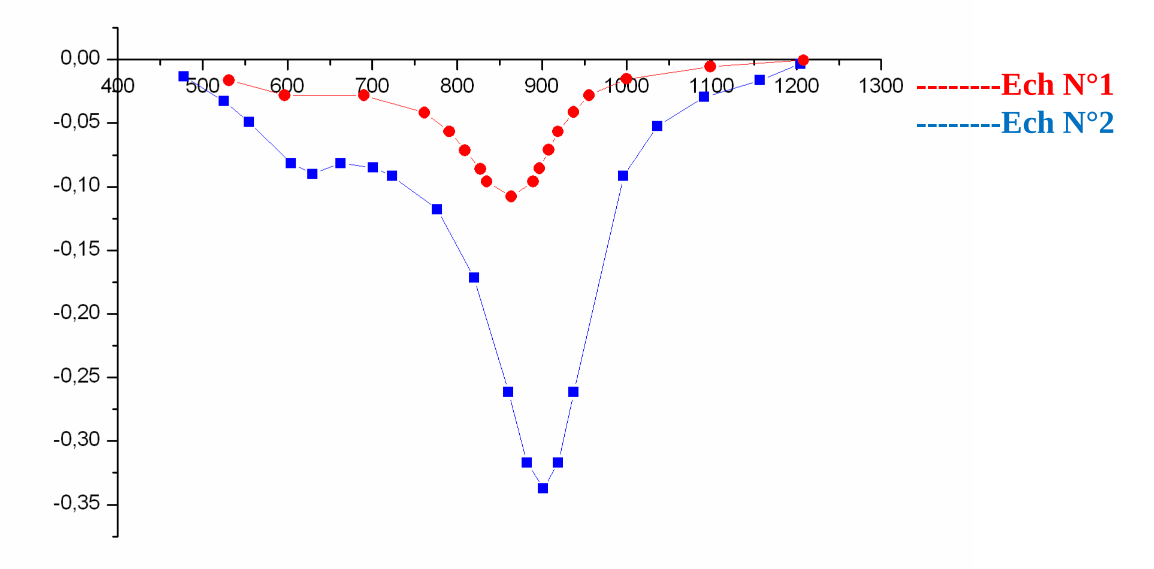
UNIVERSITY HASSAN II OF CASABLANCA
FACULTY OF SCIENCES BEN M'SIK
DEPARTMENT OF CHEMISTRY

UNIVERSITY ANNUAL 2018-2019

Master Materials Engineering and Energy
Module : **Ceramics and Glass**
Semestre 2
Pr. Saïd BENMOKHTAR

Control (5)

1) Vous devez réaliser la synthèse dans l'état solide et à haute température de la céramique de formule $NaZr_2(PO_4)_3$.
Ecrivez et équilibrez la réaction chimique.
2) le frittage
a) est un procédé de granulation des poudres en général
b) est un procédé de granulation spécifique de certaine poudre
c) sert à réduire les espaces inter granulaires de certains type de poudres
d) a + b + c
e) b + c
3) Quelles informations apportent la dilatomètrie ?
Les dérivés des courbes dilatométriques des deux échantillons $NaZr_2(PO_4)_3$, et $KZr_2(PO_4)_3$ en fonction de la température de frittage permettent de suivre la vitesse de retrait en fonction de la température.



UNIVERSITY HASSAN II OF CASABLANCA
FACULTY OF SCIENCES BEN M'SIK
DEPARTMENT OF CHEMISTRY

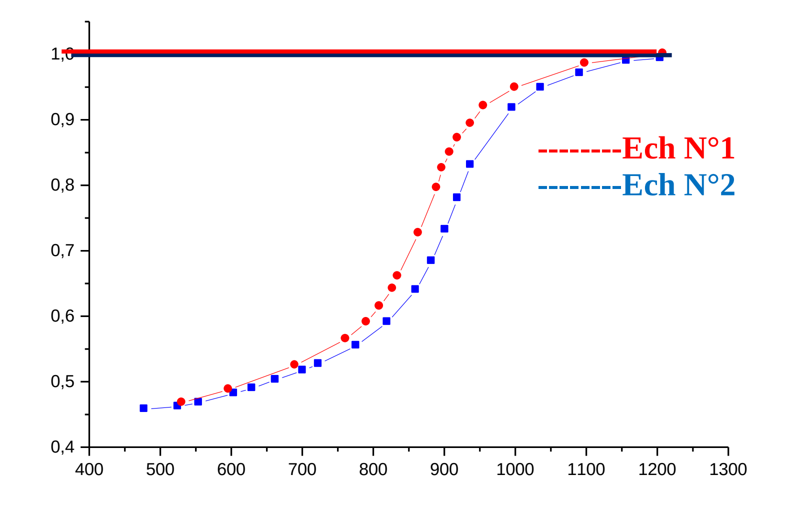
UNIVERSITY ANNUAL 2018-2019

Master Materials Engineering and Energy
Module : **Ceramics and Glass**
Semestre 2
Pr. Saïd BENMOKHTAR

Control (6)

1) Vous devez réaliser la synthèse dans l'état solide et à haute température de la céramique de formule $KZr_2(PO_4)_3$.
Ecrivez et équilibrez la réaction chimique.
2) Donner un mécanisme de frittage en phase solide i) avec retrait et ii) sans retrait
3) Décrire la différence entre «pressé» et «isostatique" dans la fabrication de la céramique.
4) Citer des modèles permettant la modélisation du frittage.
Quelles informations apportent la dilatomètrie ?
5) Pour l'étude par dilatomètrie on utilise la formule ci dessous pour exprimer l'état de densification instantané pendant le frittage
5-a) Donner la signification de chaque terme.
5-b) Démontrez cette formule (supposition retrait isotrope)

$$\frac{dD}{dt}\left(\frac{1}{D}\right) = -\frac{3}{L} \times \frac{dL}{dt}$$



UNIVERSITY HASSAN II OF CASABLANCA
FACULTY OF SCIENCES BEN M'SIK
DEPARTMENT OF CHEMISTRY
UNIVERSITY ANNUAL 2018-2019

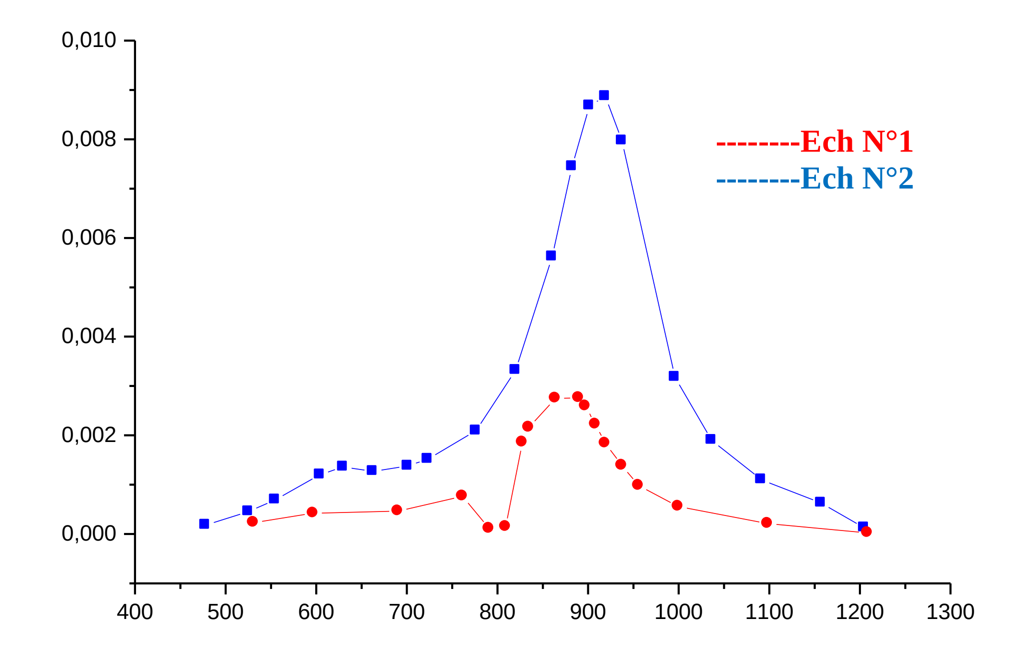
Master Materials Engineering and Energy
Module : **Ceramics and Glass**
Semestre 2
Pr. Saïd BENMOKHTAR

Control (7)

1) Donner un mécanisme de frittage en phase solide i) avec retrait et ii) sans retrait
2) Décrire la différence entre «pressé» et «isostatique" dans la fabrication de la céramique.
3) Citer des modèles permettant la modélisation du frittage.

Influence de la vitesse de chauffe sur la vitesse de densification

Les dérivés des courbes de la densité en fonction de la température de frittage des deux échantillons $NaZr_2(PO_4)_3$, et $KZr_2(PO_4)_3$



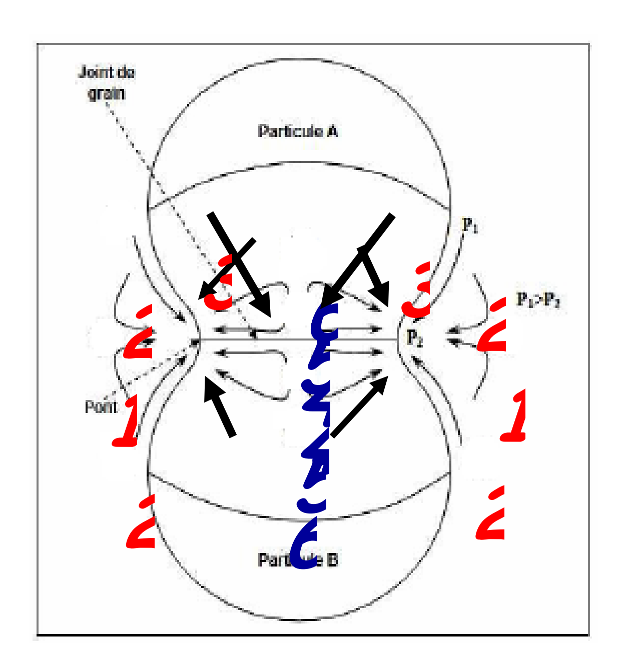
UNIVERSITY HASSAN II OF CASABLANCA
FACULTY OF SCIENCES BEN M'SIK
DEPARTMENT OF CHEMISTRY

UNIVERSITY ANNUAL 2018-2019

Master Materials Engineering and Energy
Module : **Ceramics and Glass**
Semestre 2
Pr. Saïd BENMOKHTAR

Control (8)

1) Expliquer ce mécanisme de diffusion lors du frittage par spark plasma



Numéro	Mécanisme de transport	Source de matière	Dépôt de matière	Densifiant
1				
2				
3				
4				
5				
6				

UNIVERSITY HASSAN II OF CASABLANCA
FACULTY OF SCIENCES BEN M'SIK
DEPARTMENT OF CHEMISTRY

UNIVERSITY ANNUAL 2018-2019

Master Materials Engineering and Energy
***Module :* Ceramics and Glass**
Semestre 2
Pr. Saïd BENMOKHTAR

Control (9)

La modélisation du frittage des céramiques s'attache surtout à décrire le comportement macroscopique d'une poudre qui ne peut être dissocié des caractéristiques microstructurales (taille de grain, porosité).
Décrire les modèles suivants :

Modèle de Frenkel

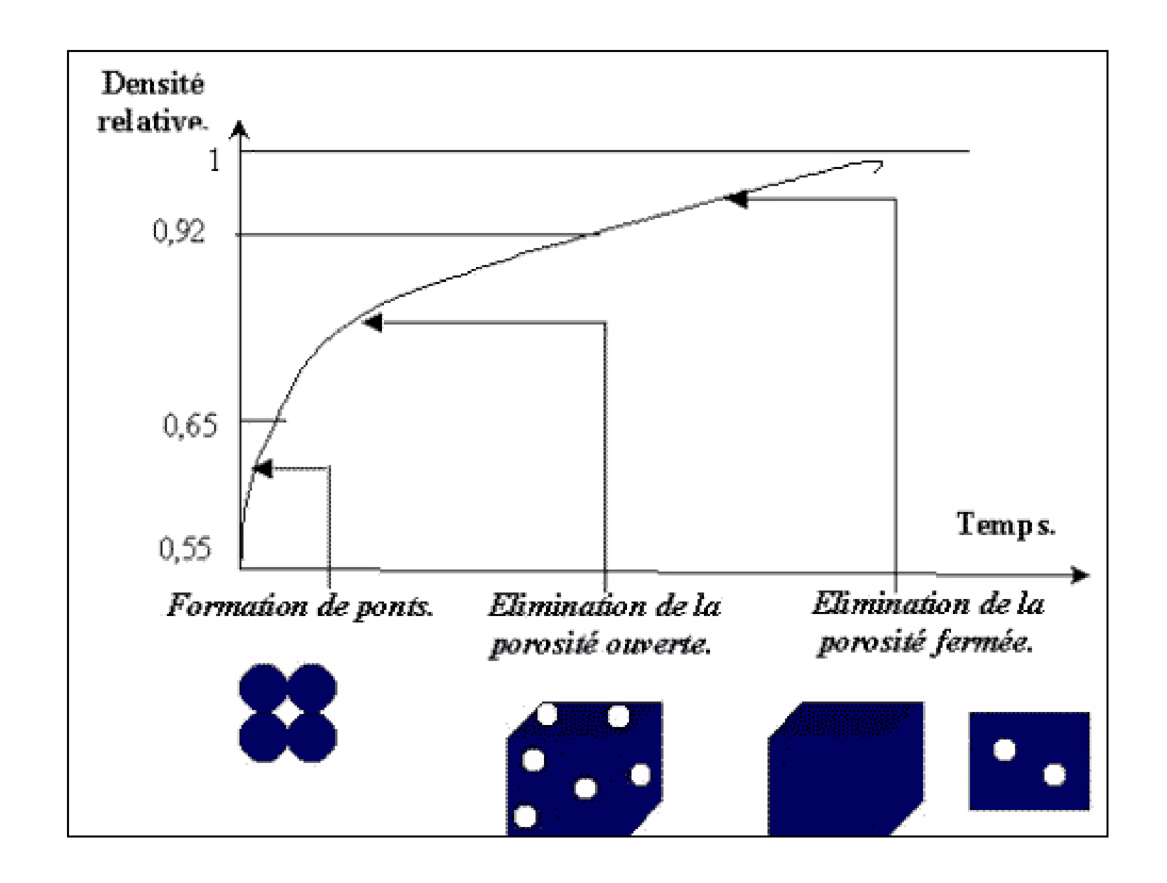
Modèle de Mackenzie-Shuttleworth

Modèle de Scherer

Modèle à clusters

Situer le domaine d'application des modèles (Frenkel, Mackenzie-Shuttleworth, Scherer)

Sur la figure suivante



UNIVERSITY HASSAN II OF CASABLANCA
FACULTY OF SCIENCES BEN M'SIK
DEPARTMENT OF CHEMISTRY

UNIVERSITY ANNUAL 2018-2019

Master Materials Engineering and Energy
Module : **Ceramics and Glass**
Semestre 2
Pr. Saïd BENMOKHTAR

Control (10)

Quel type d'informations apporte la figure 1 ?
Quel type d'informations apporte la microscopie électronique à balayage (figure 2)?
Quelles informations apporte l'analyse thermique différentielle ?
Citer des modèles permettant la modélisation du frittage.

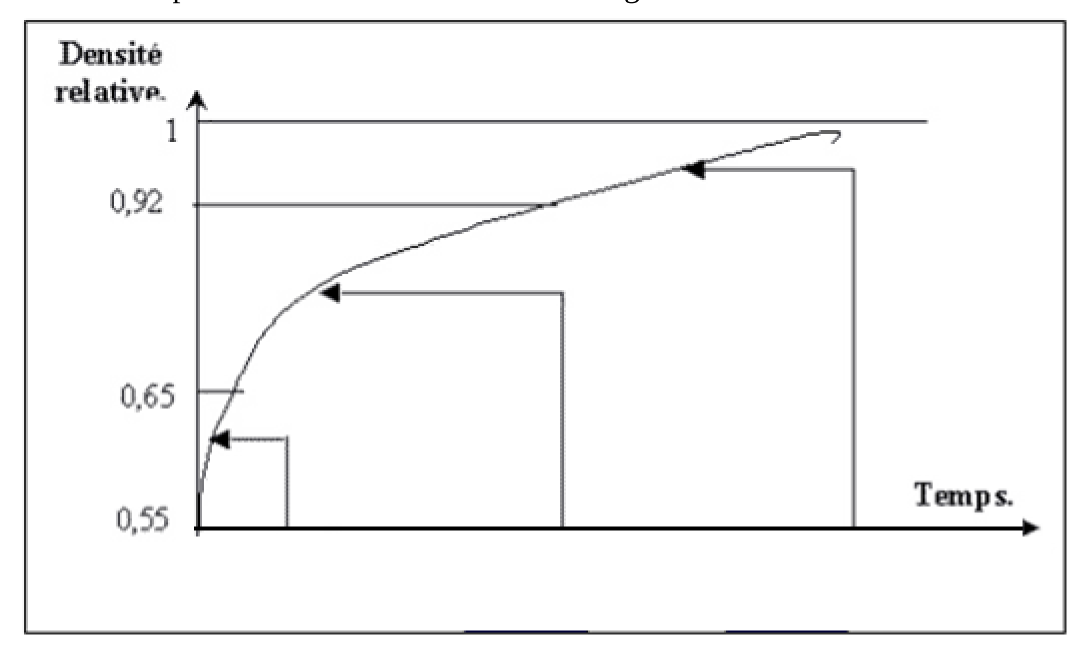


Figure 1



Figure 2

Quel type d'informations apporte la microscope électronique à balayage ?
Quelles informations apporte l'analyse thermique différentielle ?
Quelle méthode doit-t-on mettre en jeu pour savoir si un matériau subit une perte de poids avec la température.

UNIVERSITY HASSAN II OF CASABLANCA
FACULTY OF SCIENCES BEN M'SIK
DEPARTMENT OF CHEMISTRY

UNIVERSITY ANNUAL 2018-2019

Master Materials Engineering and Energy
Module : **Ceramics and Glass**
Semestre 2
Pr. Saïd BENMOKHTAR

Control (11)

1) Vous devez réaliser la synthèse dans l'état solide et à haute température de la céramique de formule $La_3Ga_5SiO_{14}$. Vous possédez les produits de départ suivants : SiO_2, Ga_2O_3 et La_2O_3.

a) Ecrivez et équilibrez la réaction chimique.
b) Déterminez les masses des oxydes de départ pour synthétiser 10g de cette céramique.

On donne les masses molaires : La : 138,91, Ga : 69,72, Si : 28,068 et O : 16

2) le frittage

a) est un procédé de granulation des poudres en général
b) est un procédé de granulation spécifique de certaine poudre
c) sert à réduire les espaces inter granulaires de certains type de poudres
d) a + b + c
e) b + c

3) Quels sont les types de frittage que l'on rencontre dans le domaine des céramiques (a) lié au mécanisme de densification et (b) le procédé technique?

4) Quelles sont les forces (énergies) motrices principales qui interviennent dans le frittage?

5) Donner un mécanisme de frittage en phase solide i) avec retrait et ii) sans retrait

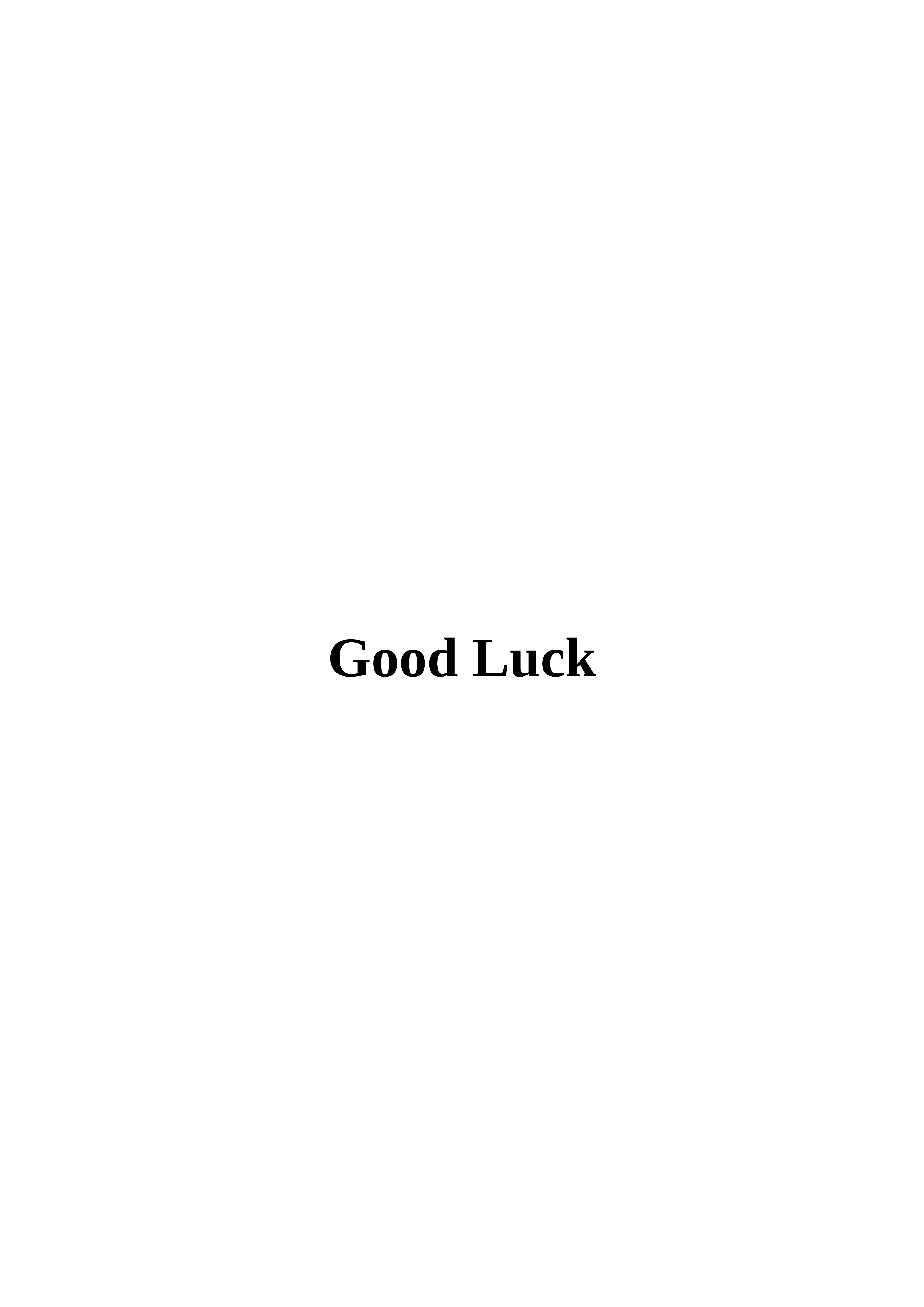
6) Décrire la différence entre «pressé» et «isostatique" dans la fabrication de la céramique.

7) Citer des modèles permettant la modélisation du frittage.

8) Expliquer dans vos propres mots qu'est-ce que la modélisation des céramiques par Monte Carlo ?

9) Quelle est la température utilisée pour le frittage d'un matériau en général? Comment peut-on diminuer cette température?

10) Donner la formule permettant de déterminer la taille des cristallites à partir de la technique de diffraction des rayons X.


Good Luck